UNIVERSITY OF OKLAHOMA

GRADUATE COLLEGE

SOME LOCAL AND GLOBAL ASPECTS OF MATHEMATICAL DIGITAL SIGNAL PROCESSING

A DISSERTATION

SUBMITTED TO THE GRADUATE FACULTY

in partial fulfillment of the requirements for the

Degree of

DOCTOR OF PHILOSOPHY

By

WEI GUAN
Norman, Oklahoma
2010

SOME LOCAL AND GLOBAL ASPECTS
OF MATHEMATICAL DIGITAL SIGNAL PROCESSING

A DISSERTATION APPROVED FOR THE
DEPARTMENT OF MATHEMATICS

BY

Dr. Meijun Zhu, Chair

Dr. John Albert

Dr. Joseph P. Havlicek

Dr. Murad Özaydin

Dr. Thordur Runolfsson

Dr. Shihshu Walter Wei

DEDICATION

to

My parents

Guan, Yongkai and Xin, Jie

For

Encouraging me to follow my dreams

Acknowledgements

My first and most earnest acknowledgement should go to my thesis advisor, Professor Meijun Zhu. In the past a few years, Professor Zhu has not only taught me a great deal of mathematics but also encouraged me in my research. All results in this thesis are joint works with Professor Meijun Zhu and I thank him for allowing me to include these results in my thesis.

I would also like to express my gratitude to Professor Murad Özaydin for his sincere and helpful advice on my studies. His Fourier transform and wavelets analysis courses were extremely valuable and beneficial to me. I would further like to thank my committee member, Professor Shihshu Walter Wei, for his unconditional support in my studies and his great help to my family. My gratitude also extends to Professor John Albert for his generosity and Professor Tomasz Przebinda for his help and support during my early career at the University of Oklahoma.

I appreciate all of the academic guidance, professional advice and financial support from Professor Joseph Havlicek and Professor Thordur Runolfsson. They were instrumental in teaching me the electrical engineering knowledge that I required for my research.

I am indebted to the department of mathematics for its direct financial support over all these years. Professor Paul Goodey deserves particular credit for his encouragement in my studies. I also would like to thank Anne Jones, Paula Killian and Gavin Nipper for their invaluable assistance.

So many friends have assisted me in many ways during my life as a graduate student in Norman that I am unable to completely express my sincere gratitude. In particular, I would like to thank Taechang Byun, Lynn Greenleaf, Catherine Hall, Nancy Ho, Suyu Li, Ye Li, Weihua Lin and Qinghua Luo.

Finally, a thank-you goes to all of my family members. Their love is the most valuable asset in my life.

Contents

Chapter 1

Introduction And Main Results

From the electric engineering field to the stock market, it is well known that an abrupt change of a signal sometimes, if not most of time, is more important to be detected. For example, a big crash or surge in stock market always easily attracts people's attention just like it is always easy to identify a few people wearing red T-shirts among a crowd with white T-shirts. The common feature in these examples is the difference or the edge. For one-dimensional signals, an abrupt change is more important to be detected from massive amount of data. The underlying philosophy is that the most important events (political, economical, etc.) usually happen around these moments. For a given image, it can be largely recognized from its edges but the map of the edges of the image requires much less storage space than the image itself since it is just a binary contour plot [1].

Edge detection usually refers to algorithms used to identify points of a signal, at which the signal values change sharply. There are many methods for edge detection, but most of them can be grouped into two categories, search-based methods, see. e.g. [2], [3], and zero-crossing based methods, see, e.g. [4], [5].

To use the search-based methods, one first needs to compute a measure of edge strength, usually a first-order derivative expression such as the gradient magnitude. Then one can search for local directional maxima of the gradient magnitude. The zero-crossing based methods search for zero crossings in a second-order derivative expression, such as the zero crossings of the Laplacian or the zero crossings of a non-linear differential expression. Thus both the search-based and the zero-crossing based edge detection methods are based on computing the discrete derivatives of the given signal. For smooth signals, it is reasonable and acceptable to view the spikes and edges as the points at which the gradient has relatively large norm or the second-order derivative equals zero. But for non-smooth signals, it does not make sense to take their derivatives.

In Chapter 2, we propose a novel approach to mathematically characterize and detect the edges of signals. The basic principles in our approach stem from the well-studied theory of nonlinear analysis, in particular from the theory of the function spaces.

The classical method to represent a signal is to express it as a function in the L^2 function space, by using Fourier transform or its variations (Wavelet transformation) [6]-[7]. The advantage of such approach is that one can easily implement algorithms based on such mathematical theory [8]. Yet, it has certain limitations. Among other things, it is not very sensitive to a rapid change of the function (for example, the derivative of the function if it is differentiable) due to the orthogonality property of different filters. For example, $sinx$ filter can only be used to determine the coefficient of $sinx$ vibration in the Fourier transform, but not for any other higher or lower vibrations. By taking into account the derivative of a given function $f(x)$ defined on an interval (a, b), one may think about representing the given function in a so called Sobolev space $W^{1,p}(a, b)$

[9], which is defined as the closure of $C^\infty(a,b)$ (all smooth functions in (a, b)) under the norm $||f||_{W^{1,p}} := ||f||_{L^p} + ||f_x||_{L^p}$, where $||f||^p_{L^p} := \int_a^b |f|^p dx$ and $||f_x||^p_{L^p} := \int_a^b |f_x|^p dx$. To capture the change of a signal, it is natural to estimate its gradient L^p energy: $||f_x||_{L^p}$. However it is not feasible to apply the theory directly in practice. For an irregular signal, it is very unstable to compute its gradient L^p norm.

The essential idea in our approach is to estimate the integral of certain function (we call it the energy) of a given signal. Based on the mathematical theory we established, one can see that the larger energy implies large gradient L^p norm for the signal. For one dimensional signal, the initial mathematical model is built on the following theorem in Chapter 2.

Theorem 2.10. *For any function* $f(x) \in W^{1,1}(0,1)$,

$$\int_0^1 e^{|f-f_A|} dx \le e^{\int_0^1 |f_x| dx},$$

where $f_A = \int_0^1 f dx$. *The constant is optimal and the equality holds if and only if* $f(x) = constant$.

Generally for $f \in W^{1,1}(a, a+\lambda)$, we can use rescaling and shifting of variable to obtain

$$\frac{1}{\lambda}\int_a^{a+\lambda} e^{|f-f_A|} dx \le e^{\int_a^{a+\lambda} |f'| dx}, \tag{1.1}$$

where $f_A = \frac{1}{\lambda}\int_a^{a+\lambda} f dx$. From inequality (1.1), we know that for a given smooth function $f(x)$ on $(a, a+\lambda)$, the large integral $\int_a^{a+\lambda} \exp\{|f - f_A|\}dx$ implies a large integral of its derivative. For a mere integrable function $f(x)$, we thus detect its abrupt change by seeking for the interval $(a, a+\lambda)$ where integral $\int_a^{a+\lambda} \exp\{|f - f_A|\}dx$ is large.

The mathematical proof of Theorem 2.10 is shown in Section 2.3.2. Based on Theorem 2.10, we develop edge detection algorithms for both one-dimensional signals and two-dimensional images in Section 2.4. We also illustrate the performance of the algorithms with examples in Section 2.4.

In Chapter 3, we study curve motions based on differential equations. Curve motion equations are classified into two types: adaptive equations (which depends on the choice of coordinate systems) and non-adaptive equations. Examples from both types of equations are studied, and the global existences for these equations are proved based on integral estimates.

Let $F(u)$: $[0,1] \to \mathbb{R}^2$ be a closed plane curve imbedded in $\mathbb{R}^2$. The evolution of $F(u)$ along its normal direction in $\mathbb{R}^2$:

$$F_t = f(k)N, \tag{1.2}$$

where N is the inner unit norm of the curve F, k is its curvature and $f(\cdot)$ is a given function, is widely studied since the early work of Gage [15] and Gage and Hamilton [16]. For $f(x) = x$, it is the well-known *curve shortening flow*. For $f(x) = x^{1/3}$, it is equivalent to the *affine curvature flow*, which was studied by Sapiro and Tannenbaum [17], and by Alvarez, et al. [18], see also, the work of Ni and Zhu [19]-[20]. Most of the studies in curve motion problems have direct impacts in digital image processing including image segment, edge detection, image denoise and many other applications [22]-[23]. We study curve motion equations like (1.2) from the view point of gradient flow of certain total energy. The study is motivated by the early work on conformal curvature flow of Ni and Zhu [19]-[20].

For any positive, 2π periodic function $\rho(\theta) \in C^2[0, 2\pi]$, and a given positive parameter α, its *α-flow constant* is defined in [19] by

$$R_\rho^\alpha = \rho^3(\alpha\rho_{\theta\theta} + \rho). \tag{1.3}$$

R_ρ^α is introduced in [19] as α-scalar curvature if ρ is given via a conformal transform, which generalizes the notion of scalar curvature as well as the affine curvature for one-dimensional curves. For instance, if $\alpha = 1$ and ρ is one-third power of the curvature of a given curve, then the 1-scalar curvature is in fact the affine curvature of the curve. The corresponding curvature flows were introduced in [19]. The global existences and the convergence of curvatures for these flows were obtained in [20]. Here we shall consider (1.3) from pure differential equation point of view. Define the average α- *flow constant* by

$$\overline{R}_\rho^\alpha = \frac{\int_0^{2\pi} \rho(\alpha\rho_{\theta\theta} + \rho)d\theta}{\int_0^{2\pi} \rho^{-2}d\theta}. \tag{1.4}$$

We introduce our motion equation as

$$\rho_t = \frac{1}{4}(R_\rho^\alpha - \overline{R}_\rho^\alpha)\rho, \qquad \text{that} \quad \text{is} \qquad \rho_t = \frac{\alpha}{4}\rho^4\rho_{\theta\theta} + \frac{1}{4}\rho^5 - \frac{1}{4}\overline{R}_\rho^\alpha\rho. \tag{1.5}$$

We will proof the following theorem.

Theorem 3.4. *For $\alpha \geq 4$, if $\rho(\theta, t)$ satisfies (1.5) with $\rho(\theta, 0) = \rho_0(\theta)$, where $\rho_0(\theta) \in C^0[0, 2\pi]$ is a positive, 2π periodic function, then $\rho(\theta, t)$ exists for all $t > 0$.*

One particular application of this theorem is to consider $\rho(\theta)$ as the polar distance for a given star-shaped polar curve: $(\theta, \rho(\theta))$. The flow may converge to its steady state $\rho(\infty)$ which has constant R_ρ^α. It is interesting to point out here that, even though a circle has constant R_ρ^α, however when $\alpha = 4$, a closed curve

$r = \rho(\theta)$ with constant R_ρ^α may not be a circle or an ellipse. See subsection 3.2.3.

The global existence and convergence of flow (1.5) for $\alpha \in (0, 4)$ are wide open, except for the case of $\alpha = 1$ and ρ satisfying certain orthogonal conditions (so that the flow is equivalent to an affine flow).

Comparing with curvature flow equations studied in [19]-[20], we classify flow (1.5) as *adaptive flows* when ρ is the polar distance functions, since the deformation of curves depends on both the shape of the figures and also the location (or coordinate systems). On the other hand, a flow which does not depend on the choice of coordinate system, such as conformal curvature flow, is classified as a *non-adaptive flow*. In particular, if ρ is given as a curvature function of a given curve in (1.5), then it is a non-adaptive flow. Unfortunately, for parameter $\alpha \neq 1$ and ρ given as a function of curvature, a closed curve may not be closed anymore under the flow (1.5).

Another family of non-adaptive flows is the following curvature flows:

$$k_t = k^2 \cdot (\tau_{\theta\theta} + \tau), \tag{1.6}$$

where $k(\theta, t)$ is the curvature and τ is a function of k. Under the flow, one can check that the orthogonal condition

$$\int_0^{2\pi} \frac{\cos\theta}{k} d\theta = \int_0^{2\pi} \frac{\sin\theta}{k} d\theta = 0 \tag{1.7}$$

holds for all $t > 0$, which guarantees that $k(\theta, t)$ is the curvature function of a closed curve. In fact, (1.6) is equivalent to the generalized curve shortening flow (1.3) with $f(k) = \tau$. From PDE point of view, we shall give another proof for the global existence when $\tau = k^p + \lambda$ for $p > 1$ and $\lambda \geq 0$.

Theorem 3.10. *Assume that $\tau = k^p + \lambda$ for $p > 1$ and $\lambda \geq 0$ in (1.6). Then solution $k(\theta, t)$ to (1.6) with $k(\theta, 0) = k_0(\theta) \in L^\infty(S^1)$ satisfying (1.7) exists for all $t > 0$.*

One can see from the isoperimetric ration that a closed curve under the normalized flow when k is the curvature function will converge to a circle.

Our approach enables us to obtain global existence to a more general adaptive flow. For any positive, 2π periodic function $\rho(\theta) \in C^2[0, 2\pi]$, and given positive parameters α and p, we define its *α-shorten-flow constant* by

$$R_p^\alpha = \rho(\alpha(\rho^p)_{\theta\theta} + \rho^p). \tag{1.8}$$

The average *α-shorten-flow constant* is given by

$$\overline{R}_p^\alpha = \frac{\int_0^{2\pi} R_p^\alpha \cdot \rho^{p-1} d\theta}{\int_0^{2\pi} \rho^{p-1} d\theta}$$

for $p \neq 1$, and

$$\overline{R}_1^\alpha = \frac{1}{2\pi} \int_0^{2\pi} R_1^\alpha d\theta$$

for $p = 1$.

Considering the normalized flow

$$\rho_t = (R_p^\alpha - \overline{R}_p^\alpha)\rho, \tag{1.9}$$

we will proof the following theorem.

Theorem 3.14. *Assume that $p > 1$ and $\alpha > 0$ in (1.9). Then for any positive function $\rho_0 \in L^\infty(S^1)$, solution $\rho(\theta, t)$ satisfying (1.9) with $\rho(\theta, 0) = \rho_0(\theta)$ exists for all $t > 0$.*

The proof of Theorem 3.14 is similar to that of Theorem 3.10. The method seems not work for $p \leq 1$. The case of $p \in [1/3, 1]$ can be settled by utilizing the proof of Theorem 3.4.

Theorem 3.17. *Assume that $p \in [1/3, 1]$ and $\alpha \geq 4$ in (1.9). Then for any positive function $\rho_0 \in L^\infty(S^1)$, solution $\rho(\theta, t)$ satisfying (1.9) with $\rho(\theta, 0) = \rho_0(\theta)$ exists for all $t > 0$.*

In fact, for $p = 1/3$, equation (1.9) is equivalent to equation (1.5).

If $\rho(\theta)$ is the polar distance for a given star-shaped polar curve: $(\theta, \rho(\theta))$, one shall expect that the curve under the flow will converge to its steady state $\rho(\infty)$, which has constant R_p^α. The rigorous proof will be discussed in the future. Based on certain Sobolev type inequalities (see Lemma 3.6), we see that the limiting shape for $\alpha \geq 4$ must be a circle; However we will present an example to show that when $\alpha < 4$, a closed curve $r = \rho(\theta)$ with constant R_p^α may not be a circle any more. The case of $\alpha = 1$ was discussed by Andrews [25].

The adaptive flows corresponding to conformal curvature flow are studied in Section 3.2 and Theorem 3.4 is proved in Section 3.2. The curve shorten flows are re-visited, and the global existence for general nonhomogeneous flow (Theorem 3.10) is proved in Section 3.3. Finally we study the adaptive flows corresponding to curve shortening flows in Section 3.4.

Chapter 2

L^p Theory On Discrete Derivative And Edge Detection

2.1 Sobolev Spaces And Inequalities

In this section, we quote some basic facts about the Sobolev spaces and Sobolev inequalities from Even's book [9].

2.1.1 Weak Derivatives

Let $U \subset \mathbb{R}^n$ be a domain and $C_0^\infty(U)$ denote the space of infinitely differentiable functions $\phi : U \to \mathbb{R}$, with compact support in U. $\alpha = (\alpha_1, \cdots, \alpha_n)$ is a multi-index of order k. That is, α_i are non-negative integers for $i = 1, \cdots, n$ and $|\alpha| = \alpha_1 + \cdots + \alpha_n = k$. Let $C^k(U)$ be the space of all $k-$th order differentiable functions and $L^1_{loc}(U)$ be the space of functions which are integrable in any compact sets of U.

For a function $u \in C^k(U)$, we define

$$D^\alpha u = \frac{\partial^{\alpha_1}}{\partial x_1^{\alpha_1}} \cdots \frac{\partial^{\alpha_n}}{\partial x_n^{\alpha_n}}(u).$$

Using integration by parts $|\alpha|$ times, we know that for a function $u \in C^k(U)$,

$$\int_U D^\alpha u \cdot \psi dx = (-1)^{|\alpha|} \int_U u \cdot D^\alpha \psi dx \tag{2.1}$$

holds for all $\psi \in C_0^\infty(U)$. We observe that the right hand side in (2.1) is well defined for any $u \in L^1_{loc}(U)$ but the expression "$D^\alpha u$" on the left hand side of (2.1) has no obvious meaning for some functions $u \in L^1_{loc}(U)$ which are not differentiable. This prompts us to introduce the definition of weak derivative.

Definition 2.1. Let $u(x) \in L^1_{loc}(U)$ and α is a multi-index. We say that u has a α-weak derivative if there is a function $v(x) \in L^1_{loc}(U)$ such that

$$\int_U u \cdot D^\alpha \psi dx = (-1)^{|\alpha|} \int_U v \cdot \psi dx \tag{2.2}$$

holds for all $\psi \in C_0^\infty(U)$. We write

$$D^\alpha u = v.$$

Example 1. Consider $U = (0, 2) \subset \mathbb{R}$ and $u \in L^1_{loc}(U)$ given by

$$u(x) = \begin{cases} x & if \quad 0 < x \leq 1 \\ 1 & if \quad 1 \leq x < 2. \end{cases}$$

We will show that u has a weak derivative given by

$$v(x) = \begin{cases} 1 & if \quad 0 < x \le 1 \\ 0 & if \quad 1 < x < 2. \end{cases}$$

To see this, we need to show that for any $\phi \in C_0^\infty(0,2)$,

$$\int_0^2 u(x)\phi'(x)dx = -\int_0^2 v(x)\phi(x)dx.$$

In fact,

$$\begin{aligned} \int_0^2 u(x)\phi'(x)dx &= \int_0^1 x\phi'(x)dx + \int_1^2 \phi'(x)dx \\ &= x\phi(x)|_0^1 - \int_0^1 \phi(x)dx + \phi(2) - \phi(1) \\ &= -\int_0^1 \phi(x)dx \\ &= -\int_0^2 v(x)\phi(x)dx. \end{aligned}$$

So $u' = v$ in the weak sense.

For some functions $u \in L^1_{loc}(U)$, the weak derivatives may not exist.

Example 2. Let $n = 1$, $U = (0,2)$ and

$$u(x) = \begin{cases} x & if \quad 0 < x \le 1 \\ 2 & if \quad 1 < x < 2. \end{cases}$$

We assert u' does not exist in the weak sense. To check this we need to show that there does not exist any function $v \in L^1_{loc}(U)$ satisfying

$$\int_0^2 u\phi' dx = -\int_0^2 v\phi dx, \tag{2.3}$$

for all $\phi \in C_0^\infty(U)$. Suppose, to the contrary, (2.3) were true for some v and all $\phi \in C_0^\infty(U)$. Then

$$\begin{aligned}
-\int_0^2 v\phi dx &= \int_0^2 u\phi' dx \\
&= \int_0^1 x\phi' dx + 2\int_1^2 \phi' dx \\
&= -\int_0^1 \phi dx - \phi(1).
\end{aligned}$$

Choose a sequence $\{\phi_m\}_{m=1}^\infty$ of smooth functions satisfying

$$0 \le \phi_m \le 1, \qquad \phi_m(1) = 1, \qquad \phi_m(x) \to 0 \qquad for\ all\ x \neq 1.$$

Replacing ϕ by ϕ_m and sending $m \to \infty$, we can find

$$1 = \lim_{m\to\infty} \phi_m(1) = \lim_{m\to\infty} (\int_0^2 v\phi_m dx - \int_0^1 \phi_m dx) = 0,$$

which is a contradiction.

Lemma 2.2. *A weak α^{th}-partial derivative of u, if it exists, is uniquely defined up to a set of measure zero.*

Proof. Assume that $v, \tilde{v} \in L^1_{loc}(U)$ satisfy

$$\int_U D^\alpha u\phi dx = (-1)^{|\alpha|} \int_U v\phi dx = (-1)^{|\alpha|} \int_U \tilde{v}\phi dx$$

for all $\phi \in C_0^\infty(U)$. Then

$$\int_U (v - \tilde{v})\phi dx = 0 \tag{2.4}$$

for all $\phi \in C_0^\infty(U)$; Hence $v - \tilde{v} = 0$ a.e. $\square$

It follows from the lemma that if a function $u \in C^k(U)$ then for $k = |\alpha|$, the regular partial derivative $D^\alpha u$ equals the weak derivative v a.e.

2.1.2 Sobolev Spaces

Fix $1 \leq p \leq \infty$ and let k be a nonnegative integer.

Definition 2.3. The Sobolev space

$$W^{k,p}(U)$$

consists of all locally integrable functions $u : U \to \mathbb{R}$ such that for each multi-index α with $|\alpha| \leq k$, $D^\alpha u$ exists in the weak sense and belongs to $L^p(U)$.

Definition 2.4. If $u \in W^{k,p}(U)$, we define its norm to be

$$\|u\|_{W^{k,p}(U)} = \begin{cases} (\sum_{|\alpha|\leq k} \int_U |D^\alpha u|^p dx)^{\frac{1}{p}} & if \quad 1 \leq p < \infty, \\ \sum_{|\alpha|\leq k} ess\ sup_U |D^\alpha u| & if \quad p = \infty. \end{cases}$$

Definition 2.5. We denote by

$$W_0^{k,p}(U)$$

the closure of $C_0^\infty(U)$ in $W^{k,p}(U)$.

Thus $u \in W_0^{k,p}$ if and only if there exist functions $u_m \in C_0^\infty(U)$ such that $u_m \to u$ in $W^{k,p}(U)$, which means $\lim_{m\to\infty} \|u_m - u\|_{W^{k,p}(U)} = 0$.

2.1.3 Sobolev Inequalities

In this section we assume $1 \leq p < n$ and we will see that for certain $1 \leq q < \infty$,

$$\|u\|_{L^q(\mathbb{R}^n)} \leq C\|Du\|_{L^p(\mathbb{R}^n)} \tag{2.5}$$

holds for all functions $u \in C_0^\infty(\mathbb{R}^n)$, where the constants $C > 0$ and q should not depend on u.

We will show that the inequality of the form (2.5) holds if q is chosen with a specific value. We first choose a function $u \in C_0^\infty(\mathbb{R}^n)$, $u \neq 0$, and define for $\lambda > 0$ the rescaled function

$$u_\lambda(x) = u(\lambda x) \qquad (x \in \mathbb{R}^n).$$

If we apply (2.5) to the rescaled function u_λ, we find

$$\|u(\lambda x)\|_{L^q(\mathbb{R}^n)} \leq C\|Du(\lambda x)\|_{L^p(\mathbb{R}^n)}. \tag{2.6}$$

Now we can change variable and set $y = \lambda x$ then

$$\begin{aligned}\|u(\lambda x)\|^q_{L^q(\mathbb{R}^n)} &= \int_{\mathbb{R}^n} |u(\lambda x)|^q dx \\ &= \frac{1}{\lambda^n}\int_{\mathbb{R}^n} |u(y)|^q dy,\end{aligned}$$

and

$$\begin{aligned}\|Du(\lambda x)\|^p_{L^p(\mathbb{R}^n)} &= \int_{\mathbb{R}^n} |Du(\lambda x)|^p dx \\ &= \frac{\lambda^p}{\lambda^n}\int_{\mathbb{R}^n} |Du(y)|^p dy.\end{aligned}$$

Inserting these equalities into (2.6), we get

$$\frac{1}{\lambda^{n/q}}\|u(x)\|_{L^q(\mathbb{R}^n)} \leq C\frac{\lambda}{\lambda^{n/p}}\|Du(x)\|_{L^p(\mathbb{R}^n)},$$

and so

$$\|u(x)\|_{L^q(\mathbb{R}^n)} \leq C\lambda^{1-\frac{n}{p}+\frac{n}{q}}\|Du(x)\|_{L^p(\mathbb{R}^n)}. \tag{2.7}$$

Thus the inequality (2.5) holds only if $1 - \frac{n}{p} + \frac{n}{q} = 0$. Otherwise we can send λ to either 0 or ∞ in (2.7) to obtain a contradiction. Thus if any inequality of the form (2.5) holds, the number q can not be arbitrary, we must necessarily have $q = \frac{np}{n-p}$.

Definition 2.6. If $1 \leq p < n$, the Sobolev conjugate of p is

$$p^* = \frac{np}{n-p}. \tag{2.8}$$

Note that

$$\frac{1}{p^*} = \frac{1}{p} - \frac{1}{n}, \qquad p^* > p.$$

The foregoing scaling analysis shows that the estimate (2.5) can only possible be true for $q = p^*$.

Theorem 2.7. *Assume $1 \leq p < n$. There exists a constant C, depending only on p and n, such that*

$$\|u\|_{L^{p^*}(\mathbb{R}^n)} \leq C\|Du\|_{L^p(\mathbb{R}^n)}, \tag{2.9}$$

for all $u \in C_0^1(\mathbb{R}^n)$.

This estimation is called Gagliardo-Nirenberg-Sobolev inequality and the detail of the proof of this theorem can be found in [9].

The next theorem follows from the Hölder inequality and the density property of $C_0^\infty(U)$ in $W_0^{1,p}(U)$.

Theorem 2.8. *Assume U is a bounded, open subset of $\mathbb{R}^n$. Suppose $u \in W_0^{1,p}(U)$ for some $1 \leq p < n$. Then we have the estimate*

$$\|u\|_{L^q(U)} \leq C\|Du\|_{L^p(U)}$$

for each $q \in [1, p^*]$, the constant C depending only on p, q, n and U.

2.2 Edge Detection And Discrete Derivative

Figure 2.1 describes the variation of natural gas price on November 11, 2007 in one hour period (courtesy of Dr. Zhen Zhu from C.H. Guernsey & Company and University of Central Oklahoma). Due to the large amount of data, we do not intent to understand all of the data. Instead, we would like to find out the moments when the price changes more dramatically.

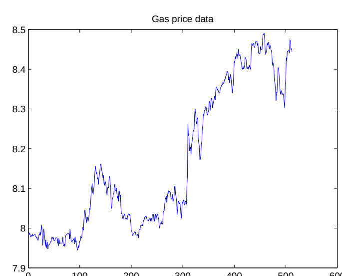

Figure 2.1: *Gas price*

A common method to capture the spikes or edges of a signal is to compute the magnitude of its discrete derivative. The large values of the magnitude will imply the spikes of the signal. There are many different ways to define the discrete derivative of one-dimensional signals [10]. Two most popular definitions are given as following.

For one-dimensional function $f(x)$ which has been sampled to produce the discrete sequence $f(i)$, for $i = 1, 2, 3, \cdots$, the discrete derivative usually is defined as either

$$\frac{\partial}{\partial x} f(x)|_{x=i} = f(i) - f(i-1), \qquad for\ i = 2, 3, 4, \cdots\ , \tag{2.10}$$

or

$$\frac{\partial}{\partial x} f(x)|_{x=i} = \frac{f(i+1) - f(i-1)}{2}, \qquad for\ i = 2, 3, 4, \cdots\ . \tag{2.11}$$

The magnitude of the derivative is correspondingly defined as

$$|\frac{\partial}{\partial x} f(x)|_{x=i} = |f(i) - f(i-1)|, \qquad for\ i = 2, 3, 4, \cdots\ ,$$

or

$$|\frac{\partial}{\partial x} f(x)|_{x=i} = |\frac{f(i+1) - f(i-1)}{2}|, \qquad for\ i = 2, 3, 4, \cdots\ .$$

Example 3. Suppose we have a signal S with length $N = 20$, and

$$S = [4, 4, 3.5, 4, 3, 4, 3, 4.5, 4, 15, 14.5, 14, 14.5, 14, 14, 14.5, 14, 14.5, 14, 14.7].$$

Then its discrete derivative

$$DS(i) = S(i) - S(i-1), \qquad for\ i = 2, 3, 4 \cdots 20.$$

Thus

$$DS = [0, -1, 1, -1, 1.5, -0.5, 11, -0.5, -0.5, 0.5, -0.5, 0, 0.5, 0.2],$$

and the magnitude of DS is

$$|DS| = [0, 1, 1, 1, 1.5, 0.5, 11, 0.5, 0.5, 0.5, 0.5, 0, 0.2].$$

From the magnitude of DS, we can easily find where the spike of the signal is. As shown in figure 2.2, the spike of the signal is around the point where the magnitude of its derivative is much bigger than that of other points. However it is challenge to find the spikes for a noised signal.

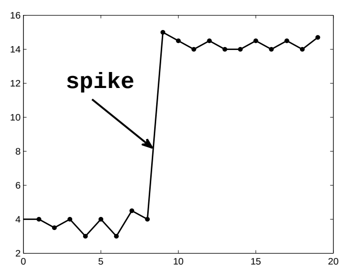

(a) *Original signal*

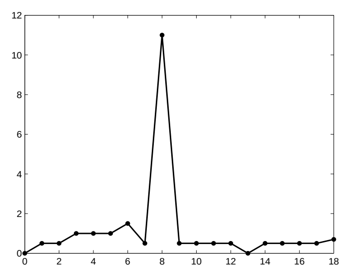

(b) *Magnitude of derivative*

Figure 2.2: *Edge of smooth signal*

Example 4. Suppose S is a noised signal with length $N = 20$ as shown in figure 2.3, and

$$S = [4, 0, 5.5, 4.8, 0.5, 1, 4, 6, 8, 10, 12, 16, 18, 15, 16, 11, 13, 15, 14, 15.5].$$

We compute the discrete derivative of this signal with two different methods defined in (2.10) and (2.11) respectively. Then

$$DS1(i) = S(i) - S(i-1), \qquad for\ 2 \leq i \leq 20,$$

and

$$DS2(i) = \frac{S(i+1) - S(i-1)}{2}, \qquad for\ 2 \leq i \leq 19.$$

The magnitudes of $DS1$ and $DS2$ are shown in figure 2.4. We can not find any

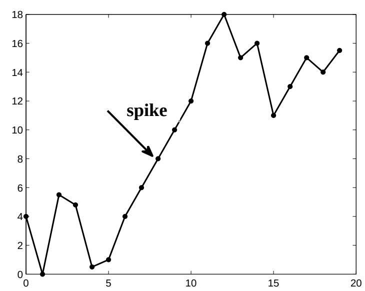

Figure 2.3: *A noised signal*

point in figure 2.4 at which the magnitude of the derivative is obviously larger than that of other points. The point, at which the magnitude of the derivative is the largest, is not the location of the spike of the signal. Thus we can not find the spike of the signal from the magnitude of its discrete derivative.

One of the reasons for this problem is that the signal has been corrupted with noise and it does not make sense to take the discrete derivative of a noised signal. In fact, even for some mathematically smooth functions, the discrete data are very unstable. Another reason is that the discrete derivative can not reflect the duration of spikes very well and it is also the reason why the spike in figure 2.3 has been missed.

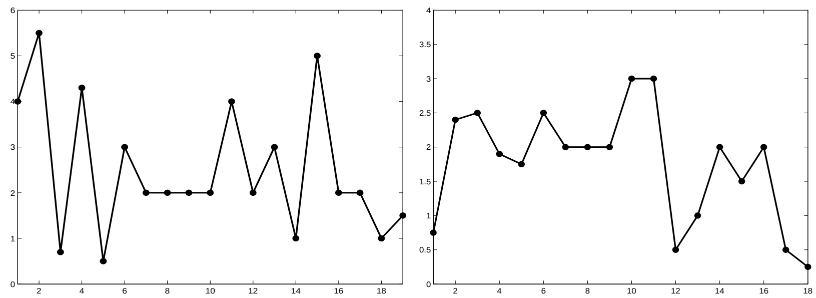

(a) *Magnitude of Ds1* (b) *Magnitude of Ds2*

Figure 2.4: *where is the spike?*

2.3 New Approach For Edge Detection

In this section, we introduce our new approach for edge detection.

2.3.1 Sobolev Type Inequalities

Let $U \subset \mathbb{R}^n$ be a bounded domain and $f(x)$ be a $n-$dimensional function defined on U. We also use the notation

$$Df(x) = (\frac{\partial f}{\partial x_1}, \cdots, \frac{\partial f}{\partial x_n}).$$

If $f_{x_i}(x)$ are all continuous, then $f(x)$ is in the function space $W^{1,p}(U)$. For $1 \leq p < n$, if $f \in W^{1,p}(U)$, then $f(x) \in L^q(U)$, for $1 \leq q \leq p^* = pn/(n-p)$. And

$$||f - f_A||_{L^q} \leq C_{q,n}||Df||_{L^p}, \tag{2.12}$$

where $C_{q,n}$ is a universal constant depending only on q and n, $f_A = \int_U |f|dx/|U| =$ average of f over U and $|Df| = \sqrt{f_{x_1}^2 + \cdots f_{x_n}^2}$.

Inequality (2.12) indicates that for a smooth function, the larger $||f - f_A||_{L^q}$ is, the larger the derivative norm $||Df||_{L^p}$ is. However $||f - f_A||_{L^q}$ is well defined for any measurable functions. This enables us to adopt a new approach to describe the edges of a digital signal.

If we want to use the L^1 norm of the derivative, $\int_U |Df|dx$, to find the spikes, we can compute $||f - f_A||_{L^q}$ for any $q \leq n/(n-1)$ locally and search for the locations where its values are relative large. But the problem is which q we should choose to compute the norm. Suppose $q_1 < q_2 < p^*$, then by Hölder inequality we have

$$\begin{aligned}
&\int_U |f|^{q_1} \cdot 1dx \\
&\leq (\int_U (|f|^{q_1})^{\frac{q_2}{q_1}} dx)^{\frac{q_1}{q_2}} \cdot (\int_U 1^{q*} dx)^{\frac{1}{q*}} \\
&\leq C(\int_U |f|^{q_2} dx)^{\frac{q_1}{q_2}},
\end{aligned}$$

where

$$q^* = \frac{q_2}{q_2 - q_1}.$$

Thus

$$\|f\|_{L^{q_1}} \leq C\|f\|_{L^{q_2}},$$

where C is a constant. By Theorem 2.8 we also have

$$\|f\|_{L^{q_2}} \leq C_{q_2,n}\|Df\|_{L^p}.$$

Thus, if the L^{q_2} norm of a function f is large then it implies that the gradient L^p norm is also large. On the other hand, it can not imply if the L^{q_1} norm of the function is large or not. If we measure the edge with the L^{q_1} norm which is small we may say it is not an spike. Thus we can capture more spikes by using L^{q_2} norm than using L^{q_1} norm.

Remark 2.9. Due to Hölder inequality, we prefer to choose q as large as possible.

However one shall be caution in dealing with one-dimensional signal because it is the case that $n = p$. From the definition of the Sobolev conjugate we know that $p^* = \frac{np}{n-p} \to +\infty$ as $p \to n$, thus we might hope that $f \in L^\infty(U)$. For $n > 1$, it is not true.

Example 5. let $U = B(0,1) \setminus \{0\}$ in $\mathbb{R}^n$, and

$$u = \ln\ln(1 + \frac{1}{|x|}).$$

Since $1 + \frac{1}{|x|}$ can go to infinity and ln is a increasing function, it is obvious that u doesn't belong to L^∞(U). If we write $r = |x|$, then for $n > 1$

$$\begin{aligned}
\int_0^1 |u_r|^n r^{n-1} dr &= \int_0^1 |\frac{1}{ln(1+\frac{1}{r})}|^n (\frac{1}{r+r^2})^n r^{n-1} dr \\
&\le \int_0^1 \frac{1}{r|lnr|^n} dr \\
&< \infty,
\end{aligned}$$

and obviously

$$\int_0^1 |u(r)|^n r^{n-1} dr < \infty.$$

Thus, we know that the function u belongs to the space $W^{1,n}$.

But for $n = 1$, it is not clear yet whether a one variable function in $W^{1,1}(U)$ will also be in $L^\infty(U)$ or not. Even if the function belongs to $L^\infty(U)$, it is still quite inaccurate to estimate its L^∞ norm if the function is discontinuous. From the definition of L^∞ norm we know that

$$\begin{aligned}\|f\|_\infty &= ess\ sup|f(t)| \\ &= inf\{M : m\{t : |f(t)| > M\} = 0\}.\end{aligned}$$

If the function is not continues, it is hard to say what is the measure of the set on which $|f(t)| > M$. In this regard, we will use the following inequality.

Theorem 2.10. *For any function $f(x) \in W^{1,1}(0,1)$,*

$$\int_0^1 e^{|f-f_A|}dx \leq e^{\int_0^1 |f_x|dx}, \tag{2.13}$$

where $f_A = \int_0^1 f dx$. The constant is optimal and the equality holds if and only if $f(x) = constant$.

2.3.2 Mathematical Proof

Proof. Let $a \in (0,1)$. We claim that: $\forall u(s) \in C^1(0,a)$ with $u(a) = 0$,

$$\int_0^a e^{|u|}ds \leq a \cdot e^{\int_0^a |u'|ds}. \tag{2.14}$$

In fact if we let $r = -\ln \frac{s}{a}$, then $dr = -\frac{1}{s}ds$ and $s = ae^{-r}$. Thus

$$\int_0^a e^{|u(s)|}ds = \int_0^\infty \frac{ae^{|u(r)|}}{e^r}dr,$$

and

$$\int_0^a |u_s|ds = \int_0^\infty |u_r|dr.$$

Moreover, $u(s)|_{s=a} = 0$ yields $u(r)|_{r=0} = 0$. It follows that

$$|u(r)| = |\int_0^r u_t dt| \leq \int_0^\infty |u_t| dt. \tag{2.15}$$

Thus

$$\int_0^\infty \frac{e^{|u(r)|}}{e^r} dr \leq e^{\{\int_0^\infty |u_t| dt\}} \cdot \int_0^\infty \frac{1}{e^r} dr = e^{\{\int_0^\infty |u_t| dt\}},$$

which yields

$$\int_0^a e^{|u|} ds \leq a \cdot e^{\int_0^\infty |u_r| dr} = a \cdot e^{\int_0^a |u_s| ds}.$$

Similarly, for $a \in (0, 1)$ we can prove that: $\forall u \in C^1(a, 1)$ with $u(a) = 0$,

$$\int_a^1 e^{|u|} ds \leq (1 - a) \cdot e^{\int_a^1 |u'| ds}. \tag{2.16}$$

Return to the proof of Theorem 2.10: first, if $f(x) \in C^1(0, 1)$ then from $\int_0^1 (f - f_A) dx = 0$, we know that there exists $a \in (0, 1)$ such that $f(a) - f_A = 0$. From (2.14) and (2.16) we have

$$\begin{aligned}
\int_0^1 e^{|f - f_A|} dx &= \int_0^a e^{|f - f_A|} dx + \int_a^1 e^{|f - f_A|} dx \\
&\leq a \cdot e^{\int_0^a |f'| dx} + (1 - a) \cdot e^{\int_a^1 |f'| dx} \\
&\leq a \cdot e^{\int_0^1 |f'| dx} + (1 - a) \cdot e^{\int_0^1 |f'| dx} \\
&= e^{\int_0^1 |f'| dx}.
\end{aligned}$$

Since $C^1(0, 1)$ is dense in $W^{1,1}(0, 1)$, (2.13) follows from standard density argument.

Note that if $f(x) = constant$, then (2.13) is an identity, thus coefficient 1 is optimal. Moreover, it is easy to see from (2.15) that the equality holds only if

$f' = 0$, that is, $f(x)$ is a constant function. $\square$

Remark 2.11. Generally for $f \in W^{1,1}(a, a+\lambda)$, we can use rescaling and shifting of variable to obtain

$$\frac{1}{\lambda} \int_a^{a+\lambda} e^{|f-f_A|} dx \leq e^{\int_a^{a+\lambda} |f'| dx}, \tag{2.17}$$

where $f_A = \frac{1}{\lambda} \int_a^{a+\lambda} f dx$. It is also clear from the proof of Theorem 2.10 that a function in $W^{1,1}(a, a+\lambda)$ is in fact in $L^\infty(a, a+\lambda)$.

From (2.17) we know that for a given smooth function $f(x)$ on $(a, a+\lambda)$, the larger is the integral $\int_a^{a+\lambda} \exp\{|f - f_A|\} dx$, the larger is the integral of its derivative. Thus the larger is the change. For a mere integrable function $f(x)$, we thus detect its abrupt changes by seeking for the intervals $(a, a+\lambda)$ where integral $\int_a^{a+\lambda} \exp\{|f - f_A|\} dx$ is large.

Remark 2.12. Using the integral of exponential function is optimal in the following sense: Sobolev-Poincaré inequality says that for any $p \in (1, +\infty)$, there is a constant $C_{p,\lambda}$ depending on p and λ such that

$$(\int_a^{a+\lambda} |f - f_A|^p dx)^{1/p} \leq C_{p,\lambda} \int_a^{a+\lambda} |f'| dx.$$

Thus, a large $||f - f_A||_{L^p}$ norm implies a large $||f'||_{L^1}$ norm and can also be used to represent a large change. On the other hand, a large integral $||f - f_A||_{L^p}$ does yield a large $\int_a^{a+\lambda} exp\{|f - f_A|\} dx$ norm, but not vice verse.

2.4 Applications In Digital Signal Processing

2.4.1 Applications In One Dimensional Signal Processing

In this section, we develop an algorithm based on the Sobolev type inequality (2.17) to detect the spikes for one-dimensional signals. we test the performance of the algorithm with some examples.

We denote the given discrete signal with $S(k)$ for $k = 1, 2, \cdots, l$, where l is the length of the signal. The algorithm is as following.

Algorithm1:

Step 1. Choose the length of spikes $n_i \in (1, l)$, $i = 1, 2, \cdots, m$.

Step 2. For each n_i, $i = 1, 2, \cdots, m$, set the $j-$th piece signal with length n_i as

$$S_{n_i}^j = (S(j), S(j+1), \cdots, S(j+n_i)), \qquad \text{for} \ \ j = 1, 2, \cdots, l - n_i.$$

Step 3. Compute the average of $S_{n_i}^j$

$$a_{n_i}(j) = \frac{1}{n_i} \sum_{k=j}^{j+n_i-1} S(k),$$

for $j = 1, 2, \cdots, l - n_i$, $i = 1, 2, \cdots, m$.

Step 4. For each piece of signal $S_{n_i}^j$, compute the the coefficient

$$C_{n_i}(j) = \frac{1}{n_i} \cdot \sum_{k=j}^{j+n_i-1} e^{|S(k) - a_{n_i}(j)|}, \tag{2.18}$$

for $j = 1, 2, \cdots, l - n_i$, $i = 1, 2, \cdots, m$.

Step 5. Choose the threshold value T and define the vectors P_{n_i} as following to indicate the intervals where the rapid changes occur.

$$P_{n_i}(j) = \begin{cases} 1 & \text{if } \ C_{n_i}(j) \geq T \\ 0 & \text{if } \ C_{n_i}(j) < T, \end{cases}$$

for all intervals $(j, j+n_i)$, where $j = 1, 2, \cdots, l - n_i$ and $i = 1, 2, \cdots, m$.

Step 6. Define the processed signal by

$$RS(j+k) = \begin{cases} S(j+k) & \text{if } \ P_{n_i}(j) > 0 \\ 0 & \text{if } \ P_{n_i}(j) = 0, \end{cases}$$

for $j = 1, \cdots, l - n_i$, $k = 0, 1, \cdots, n_i$ and $i = 1, 2, \cdots, m$.

In this algorithm, the length of each piece of signal, the value of n_i, certainly affects the outcome of computation. For relative stable result, we require that n_i can not be too small in applications.

In fact, we can modify the coefficients in (2.18) and make the spikes with different sizes more comparable. Without loss of generality, we assume that $n_1 < n_2 < \cdots < n_m$. For all n_i, $i = 1, \cdots, m$, we define

$$C^m_{n_i}(j) = (\frac{1}{n_i} \cdot \sum_{k=j}^{j+n_i-1} e^{S(k) - a_{n_i}(j)})^{\frac{n_m}{n_i}}, \tag{2.19}$$

for $j = 1, 2, \cdots, l - n_i$ and $i = 1, 2, \cdots, m$. We then threshold among all coefficients

$$\{C^m_{n_1}(j)\}_{j=1}^{l-n_1}, \{C^m_{n_2}(j)\}_{j=1}^{l-n_2}, \cdots, \{C^m_{n_m}(j)\}_{j=1}^{l-n_m}.$$

Now we test the performance of algorithm 1 with some examples. We analyze the natural gas price data which has been shown in figure 2.1. In all figures, we show the original signal with dot line and the detected spikes with solid line.

Example 6. We first test the effect of changing the threshold value. Let $n = 8$ and compute the coefficients $C_n(j)$ in (2.18). We take the maximum of the coefficients as the threshold value T and show the detected spike in figure 2.5 (a). Then we change the threshold value T properly such that 1% coefficients are larger than the threshold value. The detected spikes are shown in figure 2.5 (b). We can see that more spikes are found.

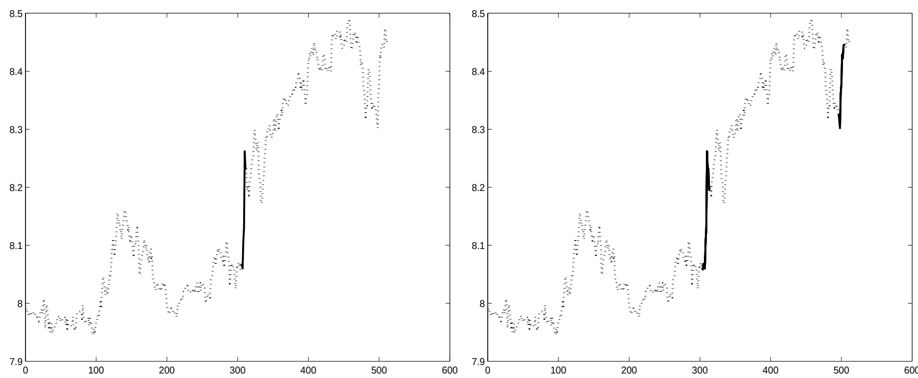

(a) keep the largest coefficient (b) Keep 1% coefficients

Figure 2.5: $n = 8$

In the following two examples we test the effect of computing different type coefficients when the length of spikes has multi-choices.

Example 7. Let $n_1 = 4$, $n_2 = 8$, $n_3 = 16$ and the threshold value T equal the maximum of the coefficients. We first compute the coefficients $C_{n_i}(j)$ in (2.18) and show the detected spike in figure 2.6 (a). We can see that the spike in figure 2.6 (a) is the same as the spike in figure 2.5 (a). It is because that the largest coefficient is one of the coefficients with $n_2 = 8$. Then we compute the coefficients $C^m_{n_i}(j)$ in (2.19) and show the detected spike in figure 2.6 (b). We still find the spike at the same location as in figure 2.6 (a) but the spike is shorter than the spike in figure 2.6 (a). The reason is that the largest coefficient among $C^m_{n_i}(j)$ is a coefficient with $n_1 = 4$. Thus we make the shorter spike are more comparable to the longer one by computing coefficients $C_{n_i}^m(j)$.

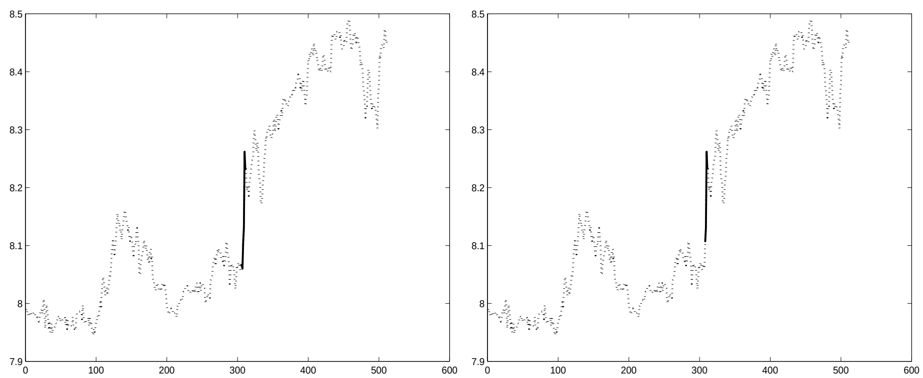

(a) Compute $C_{n_i}(j)$ (b) Compute $C_{n_i}^m(j)$

Figure 2.6: *Let* $n_1 = 4, n_2 = 8, n_3 = 16$ *and only keep the largest coefficient*

Example 8. Let $n_1 = 4$, $n_2 = 8$, $n_3 = 16$. In this example, we choose the threshold value T properly such that 4 coefficients are larger than the threshold value. We first compute the coefficients $C_{n_i}(j)$ in (2.18) and show the detected spikes in figure 2.7 (a). It looks that there is only one spike in figure 2.7 (a) but the spike is longer than the spike in figure 2.6 (a). The reason is that we find more spikes that are overlap with each other. We then compute coefficients $C_{n_i}^m(j)$ in (2.19) and show the detected spikes in figure 2.7 (b). In this case, we find spikes at two different locations.

From these examples, we can see how the threshold value,the length of spikes and the different type coefficients affect spike detection results.

2.4.2 Applications In Image Edge Detection

The edges of an image are the sudden, sustained changes in average image intensity that extend along a contour [10]. The purpose of detecting the edges of an image is to capture the important information and structure of the image.

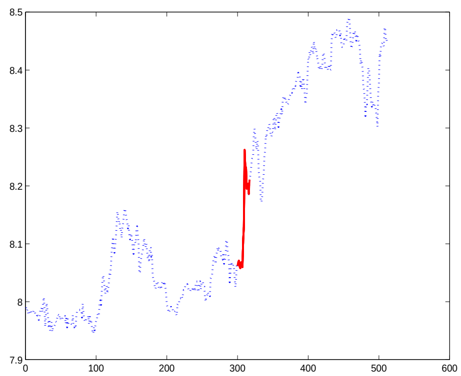

(a) Compute $C_{n_i}(j)$ (b) Compute $C_{n_i}^m(j)$

Figure 2.7: *Let* $n_1 = 4, n_2 = 8, n_3 = 16$ *and keep 4 large coefficients*

There are many edge detection methods, but most of them are based on computing the discrete derivatives of images. In this section, we develop an edge detection algorithm which is based on the Sobolev type inequality in Theorem 2.10.

For a $N \times M$ image $I(i,j)$, $\ i = 1, 2, \cdots, N$, $j = 1, 2, \cdots, M$, we view each row and each column of the image as one-dimensional signals and cut them into small pieces. The algorithm is following.

Algorithm 2.

step1. Choose a value n with $n < N$ and $n < M$, which is the length of each small piece of signal.

step2. Set $ax(i,j) = \frac{1}{n}\sum_{k=j}^{j+n-1} I(i,k)$, and $bx(i,j) = \frac{1}{n}\sum_{k=j}^{j+n-1} e^{|I(i,k)-ax(i,j)|}$, for $i = 1, 2, \cdots, N$, $j = 1, 2, \cdots, M-n$.

step3. Set $ay(i,j) = \frac{1}{n}\sum_{k=i}^{i+n-1} I(k,j)$, and $by(i,j) = \frac{1}{n}\sum_{k=i}^{i+n-1} e^{|I(k,j)-ay(i,j)|}$, for $i = 1, 2, \cdots, N-n$, $j = 1, 2, \cdots, M$.

step4. Set $b(i,j) = \sqrt{bx(i,j)^2 + by(i,j)^2}$, for $i = 1, 2, \cdots, N-n$, $j = 1, 2, \cdots, M-n$.

step5. Choose the threshold value T and define the edge function e as :

$$e(i,j) = \begin{cases} 1 & if \quad b(i,j) \geq T \\ 0 & if \quad b(i,j) < T, \end{cases}$$

for $i = 1, 2, \cdots, N-n$, $j = 1, 2, \cdots, M-n$.

In this algorithm, the detected edges may be thick due to the large value of n. Thus we can apply an edge thinning process if needed and modify algorithm 2 by setting the edge function $\hat{e}$ as following,

$$\hat{e}(i,j) = \begin{cases} 1 & if \quad b(i,j) \geq T, b(i-1,j) < T, b(i,j-1) < T \\ 0 & otherwise, \end{cases}$$

for $i = 1, 2, \cdots, N-n$, $j = 1, 2, \cdots, M-n$.

We now test the performance of algorithm 2 with some examples. We first use algorithm 2 to process some simple images in figure 2.8 and we indicate the detected edge locations using white contours in the map of edges(edge-map).

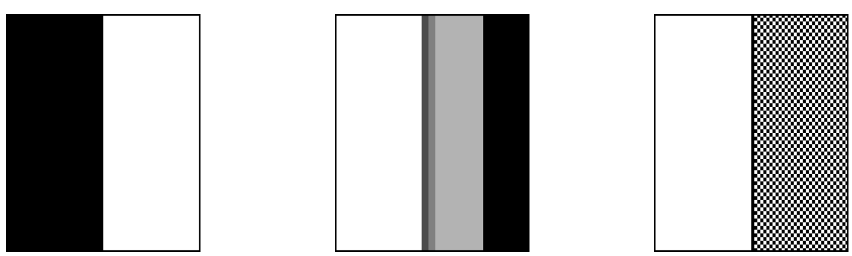

(a) Image A (b) Image B (c) Image C

Figure 2.8: *where are the edges?*

Example 9. We first let $n = 3$ and the threshold value $T = 0$. The edge-maps are shown in figure 2.9. From these edge-maps, we can see that we find the edge in

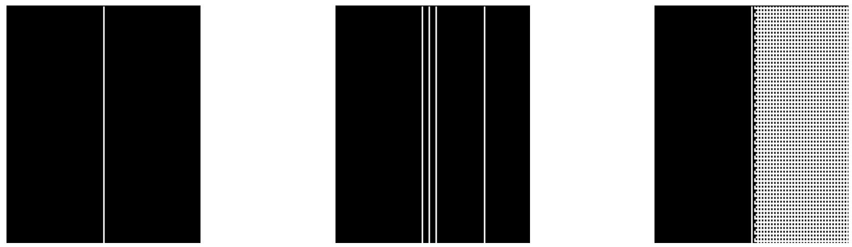

(a) Edge-map A (b) Edge-map B (c) Edge-map C

Figure 2.9: *Small scale edges*

the middle of image A and four edges in image B. For image C, we find the edge in the middle of the image and a lots of small edges on the right half part of the image.

Example 10. Now we let $n = 10$, $T = 0$ and we apply the edge thinning process to detected edges. The edge-maps are shown in figure 2.10. The edge in the

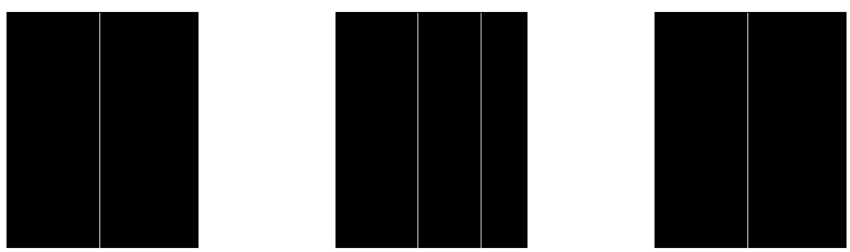

(a) Edge-map A (b) Edge-map B (c) Edge-map C

Figure 2.10: *large scale edges*

middle of image A and the edge in the middle of image C are detected. Only two edges are detected in image B. Some edges in image B and image C are missed due to the larger value of n.

Example 11. In this example, we let $n = 3$, but we increase the threshold value of each image to the average of the coefficients matrix b. The edge-maps are shown

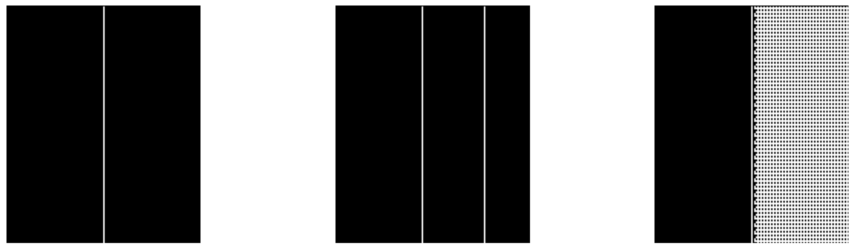

(a) Edge-map A (b) Edge-map B (c) Edge-map C

Figure 2.11: *Sharper small scale edges*

in figure 2.11. We find the edge in the middle of image A, the edge in the middle of image C and a lots of small edges on the right part of image C because all of them are the edges between black and white, the sharpest edge for gray images. For image B, two edges are blocked by the higher threshold value because they are not considered as an edge under the higher threshold value.

From these examples, we can see that we can use algorithm 2 to detect different type edges by adjusting the value n and T. Before we process some more typical images with algorithm 2, we introduce three common edge detection operators: Roberts operator, Prewitt operator and Sobel operator. All these edge detection operators are based on computing the partial discrete derivatives of images.

For a $N \times N$ gray image $I(i,j)$, $i,j = 1,2,3,\cdots,N$, the Roberts operator is defined as

$$R(i,j) = \sqrt{(I(i,j) - I(i+1,j+1))^2 + (I(i,j+1) - I(i+1,j))^2},$$

for $i,j = 1,2,\cdots,N$. In the implementation of Roberts operator, two templates are introduced as following:

$$\begin{pmatrix} 1 & 0 \\ 0 & -1 \end{pmatrix}, \qquad \begin{pmatrix} 0 & 1 \\ -1 & 0 \end{pmatrix}. \tag{2.20}$$

To detect edges with Roberts operator, we first compute the two-dimensional convolution of the image and these two matrices respectively and get two matrices $M1$, $M2$. Then we can get the matrix R by setting

$$R(i,j) = \sqrt{M1(i,j)^2 + M1(i,j)^2}, \qquad for \qquad i,j = 1,2,3,\cdots,N.$$

We threshold the matrix R to produce the edge-map of the given image. Similar to Roberts operator, the Prewitt operator can be implemented with the following templates:

$$\begin{pmatrix} -1 & -1 & -1 \\ 0 & 0 & 0 \\ 1 & 1 & 1 \end{pmatrix}, \qquad \begin{pmatrix} -1 & 0 & 1 \\ -1 & 0 & 1 \\ -1 & 0 & 1 \end{pmatrix}. \tag{2.21}$$

For Sobel operator, the templates are

$$\begin{pmatrix} -1 & -2 & -1 \\ 0 & 0 & 0 \\ 1 & 2 & 1 \end{pmatrix}, \qquad \begin{pmatrix} -1 & 0 & 1 \\ -2 & 0 & 2 \\ -1 & 0 & 1 \end{pmatrix}. \tag{2.22}$$

In applications, the Prewitt operator and Sobel operator are not as sensitive to noise as Roberts operator because they average the estimations of $\frac{\partial}{\partial x}$ and $\frac{\partial}{\partial y}$ along three rows and columns respectively.

The image processing toolbox of Matlab 7.9.0 provides a function for image edge detection and the syntax is as following:

BW = edge(I,‘method’);

BW = edge(I,‘method’,thresh);

BW = edge(I,‘method’,thresh,direction).

The parameter ‘method’ can be chosen as edge detection operators including Roberts operator, Prewitt operator or Sobel operator. Now we use the command BW = edge(I,‘method’) and different operators to process the camera man image. The edge-maps are shown in figure 2.12. From these edge-maps we can see that

(a) Original camera man

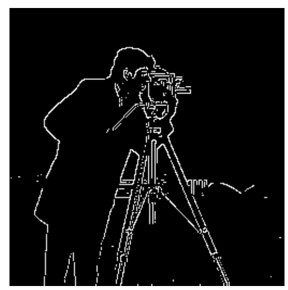

(b) Roberts operator

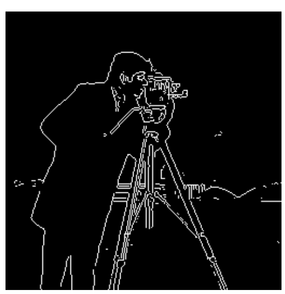

(c) Prewitt operator

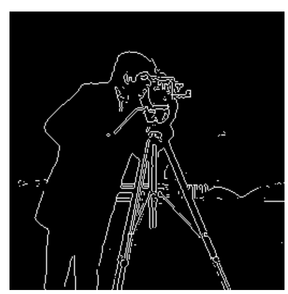

(d) Sobel operator

Figure 2.12: *Edge detection with different operators*

these three operators have very similar edge detection results for a smooth image.

We process the camera man image with algorithm 2 and compare the performance of algorithm 2 with that of those edge detection operators.

Example 12. We first let $n = 2$ and the threshold value T equal the average of the coefficients matrix b. The edge-map is shown in figure 2.13 (a). We then change the value of n to 4 but still choose the average of the coefficients matrix b as the threshold value. The edge-map is shown in figure 2.13 (b). The edges in figure 2.13 (b) are thick since $n = 4$ and no edge thinning process is applied to the detected edges.

(a) n=2 (b) n=4

Figure 2.13: *Edge detection with algorithm 2*

Now we test the performance of these edge detection operators and algorithm 2 for noised images.

Example 13. Figure 2.14 (a) is the camera man image which has been corrupted with a Gaussian noise. The mean of the noise is 0 and the variance is 0.05. Figure 2.14 (b), (c) and (d) are the edge-maps produced by Roberts operator, Prewitt operator and Sobel operator respectively. From these edge-maps, we can see that for a noised image, the Prewitt operator and Sobel operator produce better edge-maps.

We process the noised camera man image in figure 2.14 (a) with algorithm 2 in the following example.

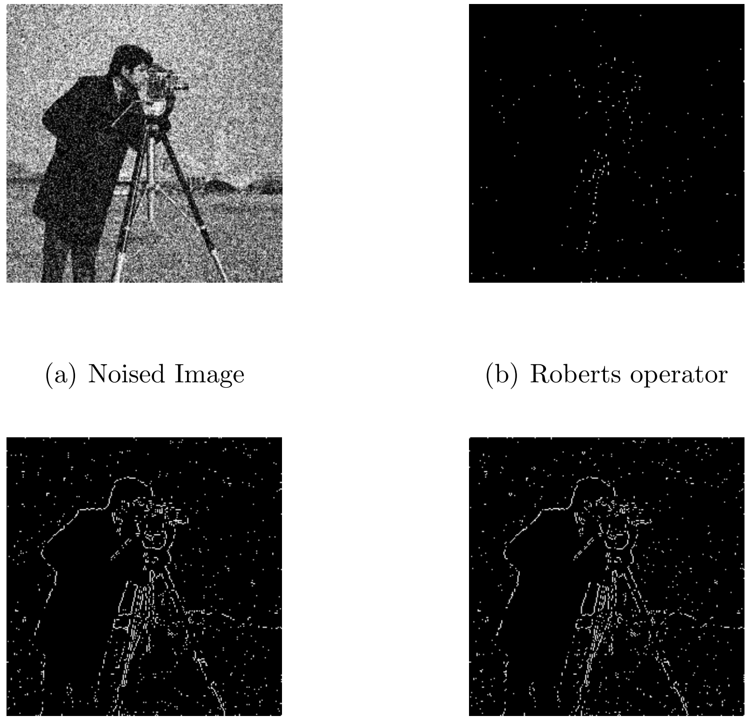

(a) Noised Image (b) Roberts operator

(c) Prewitt operator (d) Sobel operator

Figure 2.14: *Edge detection for noised image*

Example 14. To process the noised images, we adjust the value of n in algorithm 2 to reduce its noise sensitivity and choose the average of the coefficients matrix b as the threshold value T. We first let $n = 3$ and show the edge-map in figure 2.15 (a). Then we change the value of n to 7 and show the edge-map in figure 2.15 (b). We can see that the algorithm 2 is sensitive to the noise very much when $n = 3$ and it produce better edge-map when $n = 7$.

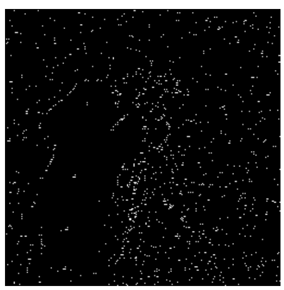

(a) Algorithm 2 with n=3

(b) Algorithm 2 with n=7

Figure 2.15: *Edge detection for noised image*

Chapter 3

Parabolic Equation Related To Curve Motion

3.1 Curvature And Curve Evolution

In this section, we quote some basic definitions related to curve motion from Do Carmo's book [14].

Definition 3.1. A parametrized differentiable plane curve is a differentiable map $F : I \to \mathbb{R}^2$ of an open interval $I = (a, b)$ of the real line $\mathbb{R}$ into $\mathbb{R}^2$.

It means that F is a correspondence which maps each $u \in I$ into a point $F(u) = (x(u), y(u)) \in \mathbb{R}^2$ and the functions $x(u), y(u)$ are differentiable. The variable u is called the parameter of the curve.

The vector$(x'(u), y'(u)) = F'(u) \in \mathbb{R}^2$ is called the tangent vector of the curve F at point u.

Definition 3.2. A parametrized differentiable plane curve $F : I \to \mathbb{R}^2$ is said to be regular if $F'(u) \neq 0$ for all $u \in I$.

Given $u \in I$, the *arc length* of a regular parametrized plane curve $F : I \to \mathbb{R}^2$ from the point u_0, is define by

$$s(u) = \int_{u_0}^{u} |F'(v)|dv, \tag{3.1}$$

where

$$|F'(v)| = \sqrt{x'(v)^2 + y'(v)^2}$$

is the length of the vector $F'(v)$.

Definition 3.3. Let $F : I \to \mathbb{R}^2$ be a plane curve parametrized by arc length $s \in I$. The number $|F''(s)| = k(s)$ is called the curvature of F at s.

Let $F(u)$: $[0, 1] \to \mathbb{R}^2$ be such a closed plane curve imbedded in $\mathbb{R}^2$, k be its curvature, $f(\cdot)$ be a given function and N be the inner unit normal vector of the curve F then the evolution of $F(u)$ along its normal direction in $\mathbb{R}^2$ is as following :

$$F_t = f(k)N. \tag{3.2}$$

If $f(x) = x$, it is the well-known *curve shortening flow* [15]. It has been proved in [16] that for the curve-shortening flow, the curvature evolves according to the equation

$$\frac{\partial k}{\partial t} = \frac{\partial^2 k}{\partial s^2} + k^3. \tag{3.3}$$

Let θ be the angle between the tangent vector and the x axis. We can use the angle θ as a universal parameter and the curvature can be written as $k = k(\theta)$. Then the equation (3.3) is equivalent to

$$\frac{\partial k}{\partial t} = k^2(\frac{\partial^2 k}{\partial \theta^2} + k). \tag{3.4}$$

It is known (see, for example [16]) that a positive 2π periodic function $k(\theta)$ represents the curvature function of a simple closed curve if and only if

$$\int_0^{2\pi} \frac{\cos\theta}{k(\theta)} d\theta = \int_0^{2\pi} \frac{\sin\theta}{k(\theta)} d\theta = 0.$$

In the rest of this chapter, we study the curve motions based on differential equations similar to (3.4). For given polar curves $(\theta, \rho(\theta))$, if the deformation of curves depends on both the shape of the figures and the location(or coordinate system), we classify it as an adaptive flow. On the other hand , if a curve flow does not depend on the choice of the coordinate system, we classify it as a non-adaptive flow. In particular, if ρ is given as a curvature function of a given curve , then it is a non-adaptive flow. We will study examples for both adaptive and non-adaptive flows.

3.2 Adaptive Flows

We first introduce an adaptive curve flow where $\rho(\theta)$ can be considered as the polar distance for a given star-shaped polar curve $(\theta, \rho(\theta))$.

For any positive, 2π periodic function $\rho(\theta) \in C^2[0, 2\pi]$, and a given positive parameter α, its *α-flow constant* is defined in [19] by

$$R_\rho^\alpha = \rho^3(\alpha\rho_{\theta\theta} + \rho). \tag{3.5}$$

Define the average α- *flow constant* by

$$\overline{R}_\rho^\alpha = \frac{\int_0^{2\pi} \rho(\alpha\rho_{\theta\theta} + \rho) d\theta}{\int_0^{2\pi} \rho^{-2} d\theta}. \tag{3.6}$$

We introduce our motion equation as

$$\rho_t = \frac{1}{4}(R^\alpha_\rho - \overline{R}^\alpha_\rho)\rho, \qquad \text{that} \quad \text{is} \qquad \rho_t = \frac{\alpha}{4}\rho^4\rho_{\theta\theta} + \frac{1}{4}\rho^5 - \frac{1}{4}\overline{R}^\alpha_\rho\rho. \tag{3.7}$$

We will show the following theorem.

Theorem 3.4. *For $\alpha \geq 4$, if $\rho(\theta, t)$ satisfies (3.7) with $\rho(\theta, 0) = \rho_0(\theta)$, where $\rho_0(\theta) \in C^0[0, 2\pi]$ is a positive, 2π periodic function, then $\rho(\theta, t)$ exists for all $t > 0$.*

3.2.1 Basic Properties

Before we derive estimates on function ρ which satisfies (3.7), we establish certain general properties of the flow for $\alpha > 0$.

In this subsection, we assume that $\rho > 0$. This assumption is satisfied by solutions to the flow with positive initial data. It is easy to see from the definition of the flow that along flow (3.7),

$$\partial_t \int_0^{2\pi} \rho^{-2} d\theta = \frac{1}{2}\int_0^{2\pi} (\overline{R}^\alpha_\rho - R^\alpha_\rho)\rho^{-2} d\theta = 0. \tag{3.8}$$

Due to this, we can assume, through the proof of Theorem 3.4, that $\int_0^{2\pi} \rho^{-2} d\theta = 2\pi$.

Lemma 3.5. *Along flow (3.7), $R := R^\alpha_\rho$ and $\overline{R} := \overline{R}^\alpha_\rho$ satisfy*

$$R_t = \frac{\alpha}{4}\rho^2(\rho^2 R_\theta)_\theta + R(R - \overline{R}), \tag{3.9}$$

and

$$\partial_t \overline{R} = \frac{1}{4\pi}\int_0^{2\pi} (R - \overline{R})^2 \rho^{-2} d\theta. \tag{3.10}$$

Proof. The proof is essentially given in [19] in the language of conformal geometry. We just re-cook the computation here:

$$\begin{aligned}
R_t =&(\rho^3(\alpha\rho_{\theta\theta}+\rho))_t = 3\rho^2\rho_t(\alpha\rho_{\theta\theta}+\rho)+\rho^3(\alpha\rho_{t\theta\theta}+\rho_t)\\
&= 3\rho^{-1}\rho_t R+\rho^3\left(\alpha(\rho\cdot\frac{\rho_t}{\rho})_{\theta\theta}+\rho\cdot\frac{\rho_t}{\rho}\right)\\
&= \frac{3}{4}(R-\overline{R})R+\alpha\rho^2(\rho^2\cdot(\frac{\rho_t}{\rho})_\theta)_\theta+R\cdot\frac{\rho_t}{\rho}\\
&= \frac{\alpha}{4}\rho^2(\rho^2 R_\theta)_\theta+R(R-\overline{R}).
\end{aligned}$$

Here, the sort of magic computation

$$\rho^3\left(\alpha(\rho\cdot\frac{\rho_t}{\rho})_{\theta\theta}+\rho\cdot\frac{\rho_t}{\rho}\right)=\alpha\rho^2(\rho^2\cdot(\frac{\rho_t}{\rho})_\theta)_\theta+R\cdot\frac{\rho_t}{\rho}$$

in facts is due to certain conformal covariant property, discovered in early work of Ni and Zhu [19] (see the proof of Proposition 1 there). Since

$$\int_0^{2\pi}\rho^{-2}d\theta=2\pi,\quad\text{and}\quad\overline{R}=\frac{1}{2\pi}\int_0^{2\pi}R\rho^{-2}d\theta,$$

we have

$$\begin{aligned}
\partial_t\overline{R} =&\frac{1}{2\pi}\int_0^{2\pi}R_t\rho^{-2}d\theta-\frac{1}{\pi}\int_0^{2\pi}R\rho^{-3}\rho_t d\theta\\
=&\frac{\alpha}{8\pi}\int_0^{2\pi}(\rho^2R_\theta)_\theta d\theta+\frac{1}{2\pi}\int_0^{2\pi}R(R-\overline{R})\rho^{-2}d\theta-\frac{1}{4\pi}\int_0^{2\pi}R(R-\overline{R})\rho^{-2}d\theta\\
=&\frac{1}{4\pi}\int_0^{2\pi}R(R-\overline{R})\rho^{-2}d\theta\\
=&\frac{1}{4\pi}\int_0^{2\pi}(R-\overline{R})^2\rho^{-2}d\theta.
\end{aligned}$$

□

From Lemma 3.5, it is clear that along flow (3.7), $\overline{R}_\rho^\alpha$ is monotonically increasing. In order to prove the global existence of the flow for certain α, we need to show that $\overline{R}_\rho^\alpha$ is bounded above for such α. In fact, for $\alpha \geq 4$, such upper bound follows from a sharp Sobolev type inequality on S^1, due to Ni and Zhu (see, e.g. Theorem 2 in [19]), and Hang [26].

Lemma 3.6. *([19], [26]) For any positive $u(\theta) \in H^1(S^1)$,*

$$\int_0^{2\pi} (u_\theta^2 - \frac{1}{4}u^2)d\theta \cdot \int_0^{2\pi} u^{-2}(\theta)d\theta \geq -\pi^2,$$

and the equality holds if and only if

$$u(\theta) = c\sqrt{\lambda^2 \cos^2 \frac{\theta - \alpha}{2} + \lambda^{-2} \sin^2 \frac{\theta - \alpha}{2}}$$

for some $\lambda, c > 0$ and $\alpha \in [0, 2\pi)$.

Corollary 3.7. *If $\alpha > 4$, then for all $u(\theta) \in H^1(S^1)$ and $u > 0$,*

$$\int_0^{2\pi} (\alpha u_\theta^2 - u^2)d\theta \cdot \int_0^{2\pi} u^{-2}(\theta)d\theta \geq -4\pi^2,$$

and the equality holds if and only if $u(\theta) = constant$.

Proof.

$$\begin{aligned}\int_0^{2\pi} (\alpha u_\theta^2 - u^2)d\theta \cdot \int_0^{2\pi} u^{-2}(\theta)d\theta &\geq -4\pi^2 + \int_0^{2\pi} (\alpha - 4)u_\theta^2 d\theta \cdot \int_0^{2\pi} u^{-2}(\theta)d\theta \\ &\geq -4\pi^2,\end{aligned}$$

and the equality holds if and only if $\int_0^{2\pi} u_\theta^2 = 0$, that is, $u(\theta) = constant$. □

From the definition of α-*flow constant*, we obtain immediately

Corollary 3.8. *(I). If $\alpha > 4$, then*

$$\overline{R}_{\rho}^{\alpha} \leq 4\pi^2,$$

and the equality holds if and only if $\rho(\theta) = constant$.

(II). If $\alpha = 4$, then

$$\overline{R}_{\rho}^{\alpha} \leq 4\pi^2,$$

and the equality holds if and only if

$$\rho(\theta) = c\sqrt{\lambda^2 \cos^2 \frac{\theta - \alpha}{2} + \lambda^{-2} \sin^2 \frac{\theta - \alpha}{2}}$$

for some $\lambda, c > 0$ and $\alpha \in [0, 2\pi)$.

3.2.2 Global Existence For $\alpha \geq 4$

We prove Theorem 3.4 in this subsection. Throughout this subsection we always assume that $\alpha \geq 4$.

Suppose that $\rho(\theta, t)$ satisfies (3.7) and $\rho(\theta, 0) = \rho_0(\theta)$, where $\rho_0(\theta)$ is a positive, 2π periodic function in $C^0(S^1)$. Then the local existence follows from the standard argument via fixed point theorem. The global existence follows from parabolic estimates and the following *a priori* estimate.

Proposition 3.9. *Suppose $\rho(\theta, t)$ satisfies (3.7) and $\rho(\theta, 0) = \rho_0(\theta)$. If $\rho_0(\theta) > 0$ and $\alpha \geq 4$, then for any given $t_0 > 0$, there is a positive constant $c = c(t_0) > 0$ such that*

$$\frac{1}{c(t_0)} \leq \rho(\theta, t) \leq c(t_0), \qquad \forall t \in [0, t_0].$$

Proof. The essential idea is the same as that in [20]. For simplicity, we use R to replace R_ρ^α and $\overline{R}$ to replace $\overline{R}_\rho^\alpha$ in the proof. From (3.9) we know that

$$R_t + \overline{R}R \geq \frac{\alpha}{4}\rho^2(\rho^2 R_\theta)_\theta.$$

It follows from the maximum principle that

$$R(\theta, t) \geq \min_\theta R(\theta, 0) \cdot e^{-\int_0^t \overline{R} d\tau}. \tag{3.11}$$

From Corollary 3.8 we know that $\overline{R} \leq 1$. Thus there is a constant $c_1(\rho_0(\theta))$ (it might be negative), depending on $\rho_0(\theta)$, such that

$$R(\theta, t) \geq c_1(\rho_0(\theta)), \qquad t \in [0, t_0]. \tag{3.12}$$

It then follows from (3.7) that there is a positive constant $c_2(\rho_0(\theta), t_0)$, depending on $\rho_0(\theta)$ and t_0, such that

$$\rho(\theta, t) = \rho_0(\theta) \cdot e^{\frac{1}{4}\int_0^t (R - \overline{R}) d\tau} \geq c_2(\rho_0(\theta), t_0) > 0, \quad t \in [0, t_0]. \tag{3.13}$$

To estimate the upper bound on $\rho(\theta, t)$, we first observe that for fixed t, ρ satisfies

$$\alpha\rho_{\theta\theta} + \rho = R\rho^{-3}, \quad \rho > 0, \quad \text{and} \quad \int_0^{2\pi} \rho^{-2} d\theta = 2\pi.$$

Multiplying the above by ρ and then integrating it from 0 to 2π, we obtain

$$\int_0^{2\pi} \rho^2 d\theta - \alpha \int_0^{2\pi} \rho_\theta^2 d\theta = \int_0^{2\pi} R\rho^{-2} d\theta = 2\pi\overline{R} \geq 2\pi\overline{R}_0, \tag{3.14}$$

where $\overline{R}_0 = \overline{R}(t)|_{t=0}$. The last inequality follows from (3.10) in Lemma 3.5. Let $M(t) = |\{\theta : \rho(\theta, t) \geq 2\}|$. Then (3.13) implies

$$2\pi = \int_0^{2\pi} \rho^{-2} d\theta = \int_{\rho \geq 2} \rho^{-2} d\theta + \int_{\rho < 2} \rho^{-2} d\theta$$
$$\leq \frac{M(t)}{4} + (2\pi - M(t)) c_2(\rho_0(\theta), t_0)^{-2}.$$

Therefore there exists $\delta(t_0) > 0$, such that $2\pi - M(t) \geq \delta(t_0)$. That is

$$|\{\theta : \rho(\theta, t) \leq 2\}| > \delta(t_0), \quad \text{for } t \in [0, t_0].$$

If $\sup_{t \in [0, t_0)} \int_0^{2\pi} \rho^2(t) d\theta = \infty$, then there exists a sequence $t_i \to t_* \leq t_0$, such that $\int_0^{2\pi} \rho^2(t_i) d\theta = \tau_i^2 \to \infty$ as $i \to \infty$. We define $v_i(\theta) = \rho(\theta, t_i)/|\tau_i|$. It follows from (3.14) that v_i satisfies

$$\int_0^{2\pi} v_i^2 d\theta = 1, \text{ and } \quad \alpha \int_0^{2\pi} (v_i)_\theta^2 d\theta \leq \int_0^{2\pi} v_i^2 d\theta - \frac{2\pi \overline{R}_0}{\tau_i^2} \leq c_3,$$

which yields that $\{v_i\}$ is a bounded set in $H^1 \hookrightarrow C^{0,\frac{1}{2}}$. Therefore up to a subsequence $v_i \rightharpoonup v_0$ in H^1 weakly and $v_0 \in C^{0,\frac{1}{2}}$. From Sobolev compact embedding we know that v_0 satisfies $\int_0^{2\pi} v_0^2 d\theta = 1$, $v_0(\theta) \geq 0$, $|\{\theta : v_0(\theta) = 0\}| \geq \delta_1(t_0) > 0$. Also, from the weak convergence $v_i \rightharpoonup v_0$ in H^1, we know that $\int_0^{2\pi} (v_0)_\theta^2 d\theta \leq \underline{\lim}_{i \to \infty} \int_0^{2\pi} (v_i)_\theta^2 d\theta$, thus

$$0 \leq \int_0^{2\pi} v_0^2 d\theta - \alpha \int_0^{2\pi} (v_0)_\theta^2 d\theta.$$

On the other hand, for an interval $I \subset (0, 2\pi)$ with positive measure if $u \in H^1(S^1)$

with $u = 0$ in I and $u \geq 0$, then for any $\alpha \geq 4$,

$$\int_0^{2\pi} u^2 d\theta - \alpha \int_0^{2\pi} (u)_\theta^2 d\theta \leq 0$$

and " = " holds if and only if $u \equiv 0$. Contradiction. Therefore $\int \rho^2 d\theta$ is bounded on $[0, t_0]$, so is $\int \rho_\theta^2 d\theta$. Thus $\rho(\theta, t)$ is bounded in $H^1 \hookrightarrow C^{0,\frac{1}{2}}$, which implies that there exists a $c(t_0) > 0$ such that

$$\frac{1}{c(t_0)} \leq \rho(\theta, t) \leq c(t_0), \qquad t \in [0, t_0].$$

□

3.2.3 Limiting Shapes

It is clear from the proof of Theorem 3.4 (in particular, from (3.13)) that $\rho(\theta, t)$ can be bounded from below by a universe positive constant independent of t_0 if the curve has initial non-negative flow constant $R(\theta, 0) \geq 0$. One could further prove that $||R - \overline{R}||_{L^\infty} \to 0$, which could yield that as $t \to \infty$, $\rho(\theta, t) \to \rho_\infty(\theta)$ with constant $\overline{R}$. It can be directly checked that the only 2π periodic solution to $\overline{R} = constant$ for $\alpha > 4$ is $\rho_\infty(\theta) = const$. Thus the limiting shape is a circle. On the other hand, for $\alpha = 4$, we know from Lemma 3.6 that $\rho_\infty(\theta)$ may not be constant. Some limiting shapes for $\alpha = 4$ are illustrated in figure 3.1.

3.3 Curve Shortening Type Flows-Revisit

A family of non-adaptive flows is the following curvature flows:

$$k_t = k^2 \cdot (\tau_{\theta\theta} + \tau) \tag{3.15}$$

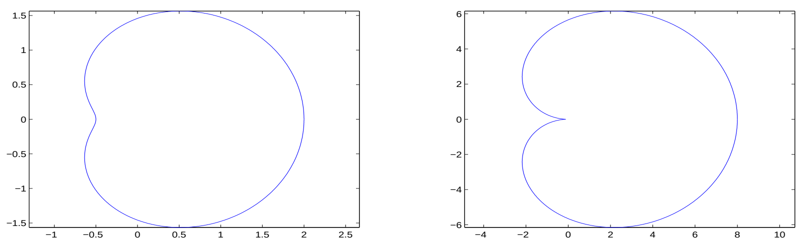

(a) *Curve* $\rho = ((\lambda^2/2 + 1/2\lambda^2) + (\lambda^2/2 - 1/2\lambda^2)cos(\theta))^{1/2}$ *for* $\lambda = 2$. (b) Curve $\rho = ((\lambda^2/2 + 1/2\lambda^2) + (\lambda^2/2 - 1/2\lambda^2)cos(\theta))^{1/2}$ for $\lambda = 8$.

Figure 3.1: *Limiting shape is not a circle for* $\lambda \neq 1$.

where $k(\theta, t)$ is the curvature and τ is a function of k. Under the flow, one can check that the orthogonal condition

$$\int_0^{2\pi} \frac{\cos\theta}{k} d\theta = \int_0^{2\pi} \frac{\sin\theta}{k} d\theta = 0 \tag{3.16}$$

holds for all $t > 0$, which guarantees that $k(\theta, t)$ is the curvature function of a closed curve. In fact, (3.15) is equivalent to the generalized curve shortening flow (3.5) with $\phi(k) = \tau$. From PDE point of view, we shall give another proof for the global existence when $\tau = k^p + \lambda$ for $p > 1$ and $\lambda \geq 0$.

Theorem 3.10. *Assume that* $\tau = k^p + \lambda$ *for* $p > 1$ *and* $\lambda \geq 0$ *in (3.15). Then solution* $k(\theta, t)$ *to (3.15) with* $k(\theta, 0) = k_0(\theta) \in L^\infty(S^1)$ *satisfying (1.7) exists for all* $t > 0$.

In order to introduce non-adaptive flows for a convex, simple closed curve F in $\mathbb{R}^2$ with curvature function $k(\theta)$ ($\theta \in [0, 2\pi]$), for the time being we introduce non-adaptive curvature $R_{\tau,\alpha}$ (similar to [19]) by

$$R_{\tau,\alpha} = k(\alpha\tau_{\theta\theta} + \tau),$$

where $\alpha > 0$ and τ is a function of k. We then introduce the following non-adaptive curve flow

$$k_t = R_{\tau,\alpha} k = k^2(\alpha\tau_{\theta\theta} + \tau). \tag{3.17}$$

However, to assure that $k(\theta, t)$ will be a curvature of a simple closed curve along the flow, we need to choose $\alpha = 1$, since only in the case of $\alpha = 1$, we have

$$\begin{aligned}
\partial_t \int_0^{2\pi} \frac{\cos\theta}{k} d\theta &= -\int_0^{2\pi} \frac{\cos\theta}{k^2} \cdot k_t d\theta \\
&= -\int_0^{2\pi} \cos\theta \cdot (\tau_{\theta\theta} + \tau) d\theta \\
&= -\int_0^{2\pi} \tau \cdot ((\cos\theta)_{\theta\theta} + \cos\theta) = 0,
\end{aligned}$$

and

$$\partial_t \int_0^{2\pi} \frac{\sin\theta}{k} d\theta = 0,$$

which guarantee that, for all $t > 0$, the orthogonal condition is preserved:

$$\int_0^{2\pi} \frac{\sin\theta}{k} d\theta = \int_0^{2\pi} \frac{\cos\theta}{k} d\theta = 0. \tag{3.18}$$

On the other hand, it can be shown (see, e.g. [16]) that flow

$$k_t = k^2(\tau_{\theta\theta} + \tau) \tag{3.19}$$

with the initial curvature satisfying (3.18) is equivalent to curve shortening flow:

$$F_t = \tau N$$

where N is the inner unit norm of the curve F.

3.3.1 Homogeneous Curve Shortening Flows

From the view point of curvature flow, we shall give a direct proof of the global existence for homogeneous curve shortening flow (i.e. $\tau = k^p$) for $p > 1$. Throughout this subsection, we always assume that $p > 1$, and use

$$R_p = k((k^p)_{\theta\theta} + k^p) \tag{3.20}$$

to represent the $p-1$-curve shortening flow curvature. The $p-1$-curvature flow is defined as:

$$k_t = R_p k.$$

Introducing the average of curvature by

$$\overline{R_p} = \frac{\int_0^{2\pi} R_p \cdot k^{p-1} d\theta}{\int_0^{2\pi} k^{p-1} d\theta}, \tag{3.21}$$

we will consider its normalized curve shortening flow:

$$k_t = (R_p - \overline{R_p})k. \tag{3.22}$$

Proposition 3.11. *For $p > 1$, if $k(\theta, t)$ satisfies (3.22) with $k_0(\theta) = k(\theta, 0) > 0$ satisfying (3.18), then $k(\theta, t) > 0$ exists for all $t > 0$.*

Proof. Again, we only need to derive the positive lower bound and upper bound for $k(\theta, t)$. From the strong Maximal Principle we know that $k(\theta, t) > 0$.

The main step in obtaining the upper bound for $k(\theta, t)$ is to show that for any given time $t_0 > 0$, $\int_0^{2\pi} k^{p-1} d\theta$, as well as $\int_0^{2\pi} [(k^p)_\theta]^2 - [k^p]^2 d\theta$ are bounded for $t \in (0, t_0)$.

We first observe that flow (3.22) preserves $\int_0^{2\pi} k^{p-1} d\theta$:

$$\partial_t \int_0^{2\pi} k^{p-1} d\theta = (p-1) \int_0^{2\pi} (R_p - \overline{R_p}) k^{p-1} d\theta = 0.$$

Without loss of generality, we can assume that $\int_0^{2\pi} k^{p-1} d\theta = 2\pi$ for all $t > 0$. It follows that for any $\delta > 0$, there is a constant $C_\delta > 0$ such that $k \leq C_\delta$ except on intervals of length less than or equal to δ. We use the assumption of $p > 1$ here.

Also, we have, along the flow, that

$$\begin{aligned}
\partial_t \int_0^{2\pi} R_p \cdot k^{p-1} d\theta &= \partial_t \int_0^{2\pi} k^p ((k^p)_{\theta\theta} + k^p) d\theta \\
&= \int_0^{2\pi} (k^p)_t ((k^p)_{\theta\theta} + k^p) d\theta + \int_0^{2\pi} k^p (((k^p)_t)_{\theta\theta} + (k^p)_t) d\theta \\
&= 2 \int_0^{2\pi} (k^p)_t ((k^p)_{\theta\theta} + k^p) d\theta \\
&= 2p \int_0^{2\pi} k^{p-1} k_t ((k^p)_{\theta\theta} + k^p) d\theta \\
&= 2p \int_0^{2\pi} (R_p - \overline{R_p}) R_p k^{p-1} d\theta \\
&= 2p \int_0^{2\pi} (R_p - \overline{R_p})^2 k^{p-1} d\theta \\
&\geq 0.
\end{aligned}$$

Note:

$$\int_0^{2\pi} R_p \cdot k^{p-1} d\theta = \int_0^{2\pi} (-[(k^p)_\theta]^2 + k^{2p}) d\theta.$$

So we know that there is a constant D depending only on k_0 such that

$$\int_0^{2\pi} (\frac{\partial (k^p)}{\partial \theta})^2 d\theta \leq \int_0^{2\pi} k^{2p} d\theta + D. \tag{3.23}$$

Finally, we follow the proof of the pointwise estimate in Gage and Hamilton

[16] to obtain the upper bound for curvature. Let $k(\psi_0) = \max_{[0,2\pi]} k(\theta)$, and $\psi \in [a,b]$ so that $k > C_\delta$ in interval (a,b) and $k(a) = C_\delta$. Then the length of $[a,b]$ is less than or equal to δ. For any $\psi \in [a,b]$,

$$
\begin{aligned}
k(\psi)^p &= k(a)^p + \int_a^\psi \frac{\partial(k^p)}{\partial\theta} d\theta \\
&\leq C_\delta^p + \sqrt{\delta}(\int_a^\psi (\frac{\partial(k^p)}{\partial\theta})^2 d\theta)^{1/2} \\
&\leq C_\delta^p + \sqrt{\delta}(\int_0^{2\pi} (\frac{\partial(k^p)}{\partial\theta})^2 d\theta)^{1/2} \\
&\leq C_\delta^p + \sqrt{\delta}(\int_0^{2\pi} k^{2p} d\theta + D)^{1/2}.
\end{aligned}
$$

It follows that for $k_{MAX} = \max_{t\in[0,2\pi]} k(\theta,t)$,

$$k_{MAX}^p \leq C_\delta^p + \sqrt{2\pi}\sqrt{\delta}k_{MAX}^p + \sqrt{2\pi\delta D}.$$

Choosing δ small enough we derive that

$$k_{MAX} < 2C_\delta + (2\delta D)^{\frac{1}{2p}}. \tag{3.24}$$

To show that k is bounded from below, we observe that

$$\overline{R_p} = \int_0^{2\pi} k^{2p} - (k^p)_\theta^2 d\theta \leq D_1. \tag{3.25}$$

Let

$$\tilde{k} = k \cdot e^{\int_0^t \overline{R_p} ds}.$$

$\tilde{k}$ satisfies

$$\tilde{k}_t = e^{-(p+1)\int_0^t \overline{R_p} ds} \cdot (\tilde{k}^2(\tilde{k}^p)_{\theta\theta} + (\tilde{k})^{p+2}).$$

The Maximal Principle yields that $\min_{\theta\in[0,2\pi]} \tilde{k}(\theta, t)$ is monotonically non-decreasing in t. Combining this with (3.24), we have: for any $t_0 > 0$,

$$k(\theta, t_0) \geq \min k_0(\theta) \cdot e^{-\int_0^{t_0} \overline{R_p} ds} \geq C(t_0). \tag{3.26}$$

From (3.24) and (3.26) we know the solution exists for all time t to equation

$$k_t = k^2(k^p)_{\theta\theta} + k^{p+2} - \overline{R_p}k,$$

which is the same as (3.22). □

We shall discuss the limiting shape under the flow at the end of this section.

Remark 3.12. The proof does not work for $p = 1$. Even though we can show that $\int_0^{2\pi} \ln k d\theta = constant$ under the normalized flow for $p = 1$, we can not show that $k(\theta)$ is bounded from below from the equation. On the other hand, we know that singularity does arise for an immersion convex curve under curve shortening flow for $p = 1$, see for example, Angenent [24].

3.3.2 Non-homogeneous Curve Shortening Flows

More generally, one considers the following non-homogenous curve shortening flow. Define the curvature

$$R_{p_\lambda} = k((k^p)_{\theta\theta} + k^p) + \lambda k = k((k^p + \lambda)_{\theta\theta} + (k^p + \lambda)),$$

where λ is a parameter. The corresponding curvature flow is given by

$$k_t = R_{p_\lambda} k = k^2((k^p)_{\theta\theta} + k^p) + \lambda k^2.$$

Define

$$\overline{R_{p_\lambda}} = \frac{\int_0^{2\pi} R_{p_\lambda} k^{p-1} d\theta}{\int_0^{2\pi} k^{p-1} d\theta}.$$

For $p > 1$ and $\lambda \geq 0$, we will show the global existence to the above flow (Theorem 3.10) via proving the global existence to the normalized flow

$$k_t = (R_{p_\lambda} - \overline{R_{p_\lambda}})k. \tag{3.27}$$

Proposition 3.13. *For $p > 1$ and $\lambda \geq 0$, if $k(\theta, t)$ satisfies (3.27) with $k_0(\theta) = k(\theta, 0) > 0$ satisfying (3.18), then $k(\theta, t) > 0$ exists for all $t > 0$.*

The proof is quite similar to that for homogeneous curve shortening flow. We shall just sketch it here.

Proof. Since $\lambda \geq 0$, from the strong Maximal Principle we know that $k(\theta, t) > 0$. Again we first observe that flow (3.27) preserves $\int_0^{2\pi} k^{p-1} d\theta$:

$$\partial_t \int_0^{2\pi} k^{p-1} d\theta = (p-1) \int_0^{2\pi} (R_{p_\lambda} - \overline{R_{p_\lambda}}) k^{p-1} d\theta = 0.$$

Without loss of generality, we assume that $\int_0^{2\pi} k^{p-1} d\theta = 2\pi$ for all $t > 0$. It follows that for any $\delta > 0$, there is a constant $C_\delta > 0$ such that $k \leq C_\delta$ except on intervals of length less than or equal to δ. The assumption of $p > 1$ is used here. Consider energy

$$F_\lambda(k) := \int_0^{2\pi} k^p((k^p)_{\theta\theta} + k^p - 2\lambda) d\theta = \int_0^{2\pi} \{k^{2p} - 2\lambda k^p - [(k^p)_\theta]^2\} d\theta.$$

Along the flow we have

$$\begin{aligned}
\partial_t F(k) &= \partial_t \int_0^{2\pi} \{k^{2p} - 2\lambda k^p - [(k^p)_\theta]^2\} d\theta \\
&= \int_0^{2\pi} \{(2pk_t k^{2p-1} - 2\lambda p k_t k^{p-1} - 2(k^p)_\theta (k^p)_{t\theta}\} d\theta \\
&= 2p \int_0^{2\pi} k_t k^{p-1} \{k^p - \lambda + (k^p)_{\theta\theta}\} d\theta \\
&= 2p \int_0^{2\pi} (R_{p_\lambda} - \overline{R_{p_\lambda}}) R_{p_\lambda} k^{p-1} d\theta \\
&= 2p \int_0^{2\pi} (R_{p_\lambda} - \overline{R_{p_\lambda}})^2 k^{p-1} d\theta \\
&\geq 0.
\end{aligned}$$

Thus, there is a constant D_2 depending only on k_0 such that

$$\int_0^{2\pi} (\frac{\partial(k^p)}{\partial\theta})^2 d\theta \leq \int_0^{2\pi} k^{2p} d\theta + D_2. \tag{3.28}$$

From here, one can show that k is bounded from above and from below by a positive constant, similar to the proof of Proposition 3.11. This yields the global existence for the flow. □

3.3.3 Limiting Shapes

If k is the curvature of a simple and closed convex curve, (3.27) is equivalent to nonhomogeneous curve shortening flow

$$F_t = (k^p - \lambda)N. \tag{3.29}$$

Let $\tau = k^p - \lambda$. Consider its geometric normalized flow

$$F_t = (\tau - \tau_a)N, \tag{3.30}$$

where $\tau_a = \int_0^L \tau ds/L = \int_0^{2\pi} k^p ds/L - \lambda$. Then it is an area-preserving flow:

$$\partial_t(area) = -\int_0^L (\tau - \tau_a)ds = 0.$$

On the other hand, we observe that

$$\begin{aligned}\partial_t(length) &= -\int_0^L (\tau - \tau_a)kds \\ &= -\int_0^L k^{p+1}ds + \frac{\int_0^L k^p ds \cdot \int_0^L kds}{L} \\ &\leq 0.\end{aligned}$$

Thus, the isoperimetric constant is decreasing along the flow, which indicate the limit shape to flow (3.30) will be a circle. However, this does not indicate that the limiting shape for flow (3.27) is also a circle. In fact, when $p = 1/3, \lambda = 0$, above argument indicates that limiting shape for (3.30) is a circle, but the limiting shape for (3.27) (which is the normalized affine curvature flow) in fact is known to be an elliptic point.

3.4 New Adaptive Flows

Our understanding of curve flow problem from curvature flow equation prompts us to consider a new adaptive flows as follows.

For any positive, 2π periodic function $\rho(\theta) \in C^2[0, 2\pi]$, and a given positive parameter α, we define its (α, τ)-*shorten-flow constant* by

$$R_\tau^\alpha(\rho) = \rho(\alpha(\tau)_{\theta\theta} + \tau),$$

where τ is a function of ρ. The average (α, τ)- *shorten-flow constant* is given by

$$\overline{R}_\tau^\alpha = \frac{\int_0^{2\pi} R_\tau^\alpha \cdot \rho^{p-1} d\theta}{\int_0^{2\pi} \rho^{p-1} d\theta}.$$

Then the new adaptive motion equation can be defined as

$$\rho_t = (R_\tau^\alpha - \overline{R}_\tau^\alpha)\rho.$$

Here we shall just focus on a concrete example: $\tau = \rho^p$ for $p > 0$, and call the corresponding (α, τ)-*shorten-flow constant* the *(α, p)-flow constant*:

$$R_p^\alpha(\rho) = \rho(\alpha(\rho^p)_{\theta\theta} + \rho^p). \tag{3.31}$$

The average *(α, p)- flow constant* is given by

$$\overline{R}_p^\alpha = \frac{\int_0^{2\pi} R_p^\alpha \cdot \rho^{p-1} d\theta}{\int_0^{2\pi} \rho^{p-1} d\theta}, \tag{3.32}$$

and the adaptive motion equation is defined as

$$\rho_t = (R_\rho^\alpha - \overline{R}_\rho^\alpha)\rho, \qquad \text{that} \quad \text{is} \qquad \rho_t = \alpha\rho^2(\rho^p)_{\theta\theta} + \rho^{p+2} - \overline{R}_p^\alpha \rho. \tag{3.33}$$

Our current methods enable us to obtain the global existence to above equation for $p \geq \frac{1}{3}$ for certain range of α.

3.4.1 The Case of $p > 1$

We first prove the following theorem.

Theorem 3.14. *For $\alpha > 0$ and $p > 1$, if $\rho(\theta, t)$ satisfies (3.33) with $\rho(\theta, 0) = \rho_0(\theta)$, where $\rho_0(\theta) \in L^\infty[0, 2\pi]$ is a positive, 2π periodic function, then $\rho(\theta, t)$ exists for all $t > 0$.*

Proof. The proof is almost the same as that of Proposition 3.11. The strong Maximal Principle yields that $\rho(\theta, t) > 0$.

First, observe that flow (3.33) preserves $\int_0^{2\pi} \rho^{p-1} d\theta$:

$$\partial_t \int_0^{2\pi} \rho^{p-1} d\theta = (p-1) \int_0^{2\pi} (R_p^\alpha - \overline{R}_p^\alpha)\rho^{p-1} d\theta = 0.$$

Without loss of generality, we can assume that $\int_0^{2\pi} \rho^{p-1} d\theta = 2\pi$ for all $t > 0$. Next, we only need to show that $\int_0^{2\pi} \alpha[(\rho^p)_\theta]^2 - [\rho^p]^2 d\theta$ are bounded for $t \in (0, t_0)$. Then, similar to the proof of Proposition 3.11, from these we can show that ρ is bounded from below and above by some positive constants for fixed time $t_0 > 0$, which yields the global existence of solution.

Along the flow, we have

$$\begin{aligned}
\partial_t \int_0^{2\pi} R_p^\alpha \cdot \rho^{p-1} d\theta &= \partial_t \int_0^{2\pi} \rho^p(\alpha(\rho^p)_{\theta\theta} + \rho^p) d\theta \\
&= \int_0^{2\pi} (\rho^p)_t(\alpha(\rho^p)_{\theta\theta} + \rho^p) d\theta + \int_0^{2\pi} \rho^p((\alpha(\rho^p)_t)_{\theta\theta} + (\rho^p)_t) d\theta \\
&= 2\int_0^{2\pi} (\rho^p)_t(\alpha(\rho^p)_{\theta\theta} + \rho^p) d\theta \\
&= 2p\int_0^{2\pi} \rho^{p-1}\rho_t(\alpha(\rho^p)_{\theta\theta} + \rho^p) d\theta \\
&= 2p\int_0^{2\pi} (R_p - \overline{R}_p^\alpha) R_p \rho^{p-1} d\theta \\
&= 2p\int_0^{2\pi} (R_p - \overline{R}_p^\alpha)^2 \rho^{p-1} d\theta \\
&\geq 0.
\end{aligned}$$

Note:

$$\int_0^{2\pi} R_p \cdot \rho^{p-1} d\theta = \int_0^{2\pi} (-\alpha[(\rho^p)_\theta]^2 + \rho^{2p}) d\theta.$$

So we know that there is a constant D_3 depending only on k_0 such that

$$\int_0^{2\pi} (\alpha[(\rho^p)_\theta]^2 - \rho^{2p}) d\theta \leq D_3.$$

$\square$

3.4.2 Limiting Shapes

Since ρ is an arbitrary positive, 2π periodic function, we can not expect to show that the flow will converge to circle via isoperimetric inequality. Rather, the limiting shapes, if the flow converges, are rather complicated. The main difficulty is due to the lack of understanding of 2π periodic positive solution following equation

$$\alpha u_{\theta\theta} + u = u^{-\frac{1}{p}} \qquad \text{on} \quad S^1. \tag{3.34}$$

It is unknown whether *constant* is the only solution. For $p > 1$ and α close to zero, we will show that most likely that there are *non-constant solutions*.

For $u \in H^1(S^1)$, we define

$$\mathcal{F}_{\alpha,p}(u) = \int_{S^1} (u^{2p} - \alpha(u^p)^2_\theta) d\theta,$$

and

$$\Gamma_{p,2\pi} = \{u \in H^1(S^1) \ : \ \int_0^{2\pi} u^{p-1} d\theta = 2\pi\}.$$

From the proof of Theorem 3.14 we know that along flow (3.33), if initial function $\rho_0 \in \Gamma_{p,2\pi}$, then $\rho \in \Gamma_{p,2\pi}$, and energy $\mathcal{F}_{\alpha,p}(\rho)$ is monotonically increasing. Moreover, we know ρ is uniformly bounded with respect to time t, thus $\mathcal{F}_{\alpha,p}(\rho)$ is bounded above. These shall imply that $\rho(\theta, t) \to \rho_*(\theta)$ in suitable sense, where

$$R_p^\alpha(\rho_*) = \overline{R}_p^\alpha = constant.$$

On the other hand, if $\rho_0 \in \Gamma_{p,2\pi}$ is not a constant, then we know that

$$\int_0^{2\pi} \rho_0^{2p} d\theta > \big(\int_0^{2\pi} \rho_0^{p-1} d\theta\big)^{\frac{2p}{p-1}} \cdot 2\pi^{\frac{p+1}{p-1}} = 2\pi.$$

Thus, there is a $\alpha_0 > 0$, such that for $\alpha \in (0, \alpha_0)$, $\mathcal{F}_{\alpha,p}(\rho) > 2\pi$, this indicates that the limit ρ_* can not be constant.

For general $\alpha \in (0, 4)$, one may find ρ_0 given by

$$\rho_0^p = c_p \sqrt{\lambda^2 \cos^2 \frac{\theta}{2} + \lambda^{-2} \sin^2 \frac{\theta}{2}},$$

for suitable $\lambda > 0$ and c_p so that $\rho_0 \in \Gamma_{p,2\pi}$ and $\mathcal{F}_{\alpha,p}(\rho) > 2\pi$. With such initial data, the limiting of ρ could not be constant if it converges. We shall not pursue the details here.

3.4.3 The Case Of $p \in [1/3, 1)$

We shall show that the proof of Proposition 3.9 can be adapted to establish

Proposition 3.15. *For $\alpha \geq 4$ and $p \in [1/3, 1)$, if $\rho(\theta, t)$ satisfies (3.33) with $\rho(\theta, 0) = \rho_0(\theta)$, where $\rho_0(\theta) \in C^1[0, 2\pi]$ is a positive, 2π periodic function, then $\rho(\theta, t)$ exists for all $t > 0$.*

Proof. Again, we only need to show that for any given $t_0 > 0$, there is a positive constant $C_4 = C_4(t_0)$ depending on t_0, such that

$$\frac{1}{C_4(t_0)} \leq \rho(\theta, t) \leq C_4(t_0).$$

Since the flow preserve $\int_0^{2\pi} \rho^{p-1} d\theta$, without loss of generality, we assume that $\int_0^{2\pi} \rho^{p-1} d\theta = 1$.

We first derive the low bound: Let

$$\tilde{\rho} = \rho \cdot e^{\int_0^t \overline{R}_p^\alpha ds}.$$

Then $\tilde{\rho}$ satisfies

$$\tilde{\rho}_t = e^{-(p+1)\int_0^t \overline{R}_p^\alpha ds} \cdot (\tilde{\rho}^2 (\tilde{\rho}^p)_{\theta\theta} + (\tilde{\rho})^{p+2}).$$

The Maximal Principle yields that $\min_{\theta \in [0,2\pi]} \tilde{k}(\theta, t)$ is monotonically non-decreasing in t, thus for any $t_0 > 0$,

$$\rho(\theta, t) \geq \min \rho_0(\theta) \cdot e^{-\int_0^{t_0} \overline{R}_p^\alpha ds}, \qquad \forall t \in [0, t_0].$$

On the other hand, since $\alpha \geq 4$, using Corollary 3.7 and Hölder inequality, we have

$$\begin{aligned} \overline{R}_p^\alpha = \int_0^{2\pi} (\rho^p)^2 - \alpha[(\rho^p)_\theta]^2 d\theta &\leq 4\pi^2 (\int_0^{2\pi} (\rho^p)^{-2} d\theta)^{-1} \\ &\leq C(\int_0^{2\pi} \rho^{p-1} d\theta)^{\frac{2p}{p-1}} \\ &= C. \end{aligned}$$

So we obtain the low bound for $\rho(\theta, t)$. To obtain the upper bound, we first observe that for all $\alpha > 0$, along the flow,

$$\partial_t \int_0^{2\pi} R_p^\alpha \cdot \rho^{p-1} d\theta = 2p \int_0^{2\pi} (R_p - \overline{R}_p^\alpha)^2 \rho^{p-1} d\theta \geq 0.$$

Thus,

$$\int_0^{2\pi} (\rho^p)^2 - \alpha[(\rho^p)_\theta]^2 d\theta \geq \overline{R}_p^\alpha(0), \tag{3.35}$$

where $\overline{R}_p^\alpha(0) = \overline{R}_p^\alpha(t)|_{t=0}$.

Similar to the proof of Proposition 3.9, since ρ is bounded from below by a positive constant and $\int_0^{2\pi} \rho^{p-1} d\theta = 1$, we know that there is a constant $\delta_1(t_0) > 0$, such that

$$|\{\theta \; : \; \rho(\theta, t) \leq 2\}| > \delta_1(t_0), \quad \text{for} \;\; t \in [0, t_0]. \tag{3.36}$$

Similar to the proof of Proposition 3.9, from (3.35) and (3.36), we can show that $\int_0^{2\pi} \rho^{2p} d\theta$ is bounded. In turn, from (3.35) we know that $\int_0^{2\pi} [(\rho^p)_\theta]^2 d\theta$ is bounded.

Thus ρ is bounded due to Sobolev embedding $H^1(S^1) \hookrightarrow C^{0,\frac{1}{2}}(S^1)$. $\square$

3.4.4 The Case Of $p = 1$

For $p = 1$, we define the average total curvature as

$$\overline{R}_1^\alpha = \int_0^{2\pi} R_1^\alpha d\theta,$$

and consider the normalized flow

$$\rho_t = (R_1^\alpha - \overline{R}_1^\alpha)\rho. \tag{3.37}$$

We will show

Proposition 3.16. *For $\alpha \geq 4$ if $\rho(\theta, t)$ satisfies (3.37) with $\rho(\theta, 0) = \rho_0(\theta)$, where $\rho_0(\theta) \in C^1[0, 2\pi]$ is a positive, 2π periodic function, then $\rho(\theta, t)$ exists for all $t > 0$.*

Proof. First, we check that

$$\partial_t \int_0^{2\pi} \ln \rho d\theta = \int_0^{2\pi} (R_1^\alpha - \overline{R}_1^\alpha) d\theta = 0.$$

Without of loss of generality,we can assume that $\int_0^{2\pi} \ln \rho d\theta = 1$. Using Corollary

3.7, we have

$$\begin{aligned}
\overline{R}_1^{\alpha} = \int_0^{2\pi} \rho^2 - \alpha\rho_\theta^2 d\theta &\leq 4\pi^2 (\int_0^{2\pi} \rho^{-2} d\theta)^{-1} \\
&\leq C(\int_0^{2\pi} \rho^{\alpha-1} d\theta)^{\frac{2\alpha}{\alpha-1}} \qquad (\text{for any } \alpha \in (1/3, 1)) \\
&\leq C \cdot exp\{\frac{1}{2\pi}\int_0^{2\pi} \ln \rho d\theta\} \\
&\leq C_1.
\end{aligned}$$

Similar to the proof of Proposition 3.15, the upper bound for $\overline{R}_1^{\alpha}$ yields the positive lower bound for ρ.

Also, along the flow,

$$\begin{aligned}
\partial_t \int_0^{2\pi} R_1^{\alpha} d\theta &= \partial_t \int_0^{2\pi} \rho(\alpha\rho_{\theta\theta} + \rho) d\theta \\
&= \int_0^{2\pi} \rho_t(\alpha\rho_{\theta\theta} + \rho) d\theta + \int_0^{2\pi} \rho(\alpha\rho_{t\theta\theta} + \rho_t) d\theta \\
&= 2\int_0^{2\pi} \rho_t(\alpha\rho_{\theta\theta} + \rho) d\theta \\
&= 2\int_0^{2\pi} (R_1 - \overline{R}_1^{\alpha}) R_1 d\theta \\
&= 2\int_0^{2\pi} (R_p - \overline{R}_p^{\alpha})^2 d\theta \\
&\geq 0.
\end{aligned}$$

Thus

$$\int_0^{2\pi} \rho^2 - \alpha\rho_\theta^2 d\theta \geq \overline{R}_p^{\alpha}(0), \tag{3.38}$$

where $\overline{R}_1^{\alpha}(0) = \overline{R}_1^{\alpha}(t)|_{t=0}$. Since ρ is bounded from below by a positive constant and $\int_0^{2pi} \ln \rho d\theta = 1$, we have

$$|\{\theta \ : \ \rho(\theta, t) \leq 2\}| > \delta_2(t_0), \quad \text{for} \ \ t \in [0, t_0] \tag{3.39}$$

for some positive constant $\delta_2(t_0)$. We then can derive the upper bound for ρ from (3.38) and (3.39). The global exsitence then follows from the standard parabolic estimates. $\square$

Combining the Proposition 3.15 and 3.16, we have the following theorem.

Theorem 3.17. *Assume that $p \in [1/3, 1]$ and $\alpha > 0$ in (3.33). Then for any positive function $\rho_0 \in L^\infty(S^1)$, solution $\rho(\theta, t)$ satisfying (3.33) with $\rho(\theta, 0) = \rho_0(\theta)$ exists for all $t > 0$.*

Remark 3.18. In fact, for $p = 1/3$, equation (3.33) is equivalent to equation (3.7)

Bibliography

[1] Zhai, L., Dong, S. and Ma, H.: Recent Methods and Applications on Image Edge Detection. 2008 international Workshop on Geoscience and Remote Sensing - Volume 01, 332-335.

[2] D. Ziou, S. Tabbone: Edge detection techniques: An overview. International Journal of Pattern Recognition and Image Analysis. 8(4):537–559, 1998.

[3] T. Lindeberg: Edge detection. in M. Hazewinkel (editor), Encyclopedia of Mathematics, Kluwer/Springer, ISBN 1402006098.

[4] T. Lindeberg (1998): Edge detection and ridge detection with automatic scale selection. International Journal of Computer Vision, 30, 2, pages 117–154.

[5] T. Lindeberg (1993): Discrete derivative approximations with scale-space properties: A basis for low-level feature extraction. J. of Mathematical Imaging and Vision, 3(4), pages 349–376.

[6] E. Stein and R. Shakarchi: Fourier Analysis, an introduction. Princeton University Press,2003.

[7] David F. Walnut: An Introduction to Wavelet Analysis. 1st edition, Birkhauser, 2002.

[8] S.K.Mitra: Digital Signal Processing, A Computer-Based Approach. 1-12. McGraw-Hill Conpanies,Inc. 2001.

[9] L.C. Evans: Partial differential equations. Graduate Studies in Mathematics, 19. American Mathematical Society, Providence, RI, 1998.

[10] Hand out of digital image processing class, Electric engineering department, University of Oklahoma, 7.4-7.16.

[11] J. Canny: A computational approach to edge detection. IEEE Trans. Pattern Analysis and Machine Intelligence, vol 8(1986), pages 679-714.

[12] LS. Davis: A survey of edge detection techniques. Computer Graphics and Image Processing, vol 4, no. 3, pp 248-260, 1975

[13] K. Engel: Real-time volume graphics. A. K. Peters, Ltd, pp. 112114,2006.

[14] M.P. Do Carmo: Differential Gemortry of Curves and Surfaces. Pearson Education,Inc. 1976

[15] Gage, M.: An isoperimetric inequality with applications to curve shortening. Duke Math. J. 50 (1983), no. 4, 1225–1229.

[16] Gage, M., Hamilton, R. S.: The heat equation shrinking convex plane curves. J. Differential Geom. 23 (1986), no. 1, 69–96.

[17] Sapiro, G., Tannenbaum, A.: On Affine Plane Curve Evolution. J. Funct. Anal., 119(1994), 79-120.

[18] Alvarez, L., Guichard, F., Lions, P. L., Morel, J. M.: Axioms and fundamental equations of image processing. *Arch. Rational Mech. Anal.* 123 (1993), no. 3, 199–257.

[19] Ni, Y., Zhu, M.: Steady states for one dimensional curvature flows. Commun. Contemp. Math. 10 (2008), no. 2, 155–179.

[20] Ni, Y., Zhu, M.: One-dimensional conformal metric flow. Adv. Math. 218 (2008), no. 4, 983–1011.

[21] Osher, S., Sethian, J.: Fronts propagating with curvature-dependent speed: algorithms based on Hamilton-Jacobi formulations. J. Comput. Phys. 79 (1988), no. 1, 12–49.

[22] Frdric Cao: Geometric Curve Evolution and Image Processing. Springer,2003.

[23] R. Mallaid, J. A. Sethlan: Image processing via level set curvature flow. Applied Mathematics, Vol. 92, pp. 7046-7050, 1995.

[24] Angenent, S.: On the formation of singularities in the curve shortening flow. J. Differential Geom. 33 (1991), no. 3, 601–633.

[25] Andrews, B.: Classification of limiting shapes for isotropic curve flows. J. Amer. Math. Soc. 16 (2003), no. 2, 443–459.

[26] Hang, F.: On the higher order conformal covariant operators on the sphere, Commun. Contemp. Math. 9 (2007), no. 3, 279–299.

[27] H.G. Barrow and J.M. Tenenbaum (1981): Interpreting line drawings as three-dimensional surfaces, Artificial Intelligence, vol 17, issues 1-3, pages 75-116.